Proteomic study identifies Aurora-A mediated regulation of alternative splicing through multiple splicing factors

Arun Prasath Damodaran, Olivia Gavard, Jean-Philippe Gagné, Malgorzata Ewa Rogalska, Amit Behera, Estefania Mancini, Giulia Bertolin, Thibault Courtheoux, Bandana Kumari, Justine Cailloce, et al.

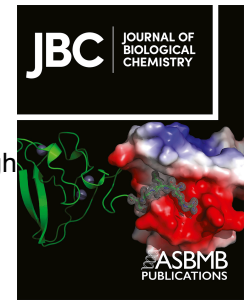

Proteomic study identifies Aurora-A mediated regulation of alternative splicing through multiple splicing factors

Arun Prasath Damodaran, Olivia Gavard, Jean-Philippe Gagné, Malgorzata Ewa Rogalska, Amit K. Behera, Estefania Mancini, Giulia Bertolin, Thibault Courtheoux, Bandana Kumari, Justine Cailloce, Agnès Mereau, Guy G. Poirier, Juan Valcárcel, Thomas Gonatopoulos-Pournatzis, Erwan Watrin, Claude Prigent

PII: S0021-9258(24)02502-X

DOI: https://doi.org/10.1016/j.jbc.2024.108000

Reference: JBC 108000

To appear in: *Journal of Biological Chemistry*

Received Date: 28 September 2023

Revised Date: 6 November 2024

Accepted Date: 8 November 2024

Please cite this article as: Prasath Damodaran A, Gavard O, Gagné JP, Rogalska ME, Behera AK, Mancini E, Bertolin G, Courtheoux T, Kumari B, Cailloce J, Mereau A, Poirier GG, Valcárcel J, Gonatopoulos-Pournatzis T, Watrin E, Prigent C, Proteomic study identifies Aurora-A mediated regulation of alternative splicing through multiple splicing factors, *Journal of Biological Chemistry* (2024), doi: https://doi.org/10.1016/j.jbc.2024.108000.

Proteomic study identifies Aurora-A mediated regulation of alternative splicing through multiple splicing factors

Arun Prasath Damodaran[1,8]*, Olivia Gavard[1], Jean-Philippe Gagné[6,7], Malgorzata Ewa Rogalska[3,4], Amit K Behera[8], Estefania Mancini[3,4], Giulia Bertolin[1], Thibault Courtheoux[1], Bandana Kumari[8], Justine Cailloce[1], Agnès Mereau[1], Guy G. Poirier[6,7], Juan Valcárcel[3,4,5], Thomas Gonatopoulos-Pournatzis[8, †], Erwan Watrin[1,†] and Claude Prigent[1,2,†]

[1] Univ Rennes, CNRS, Institut de Génétique et Développement de Rennes (IGDR) UMR6290, Équipe labellisée LNCC 2014, F-35000 Rennes, France.
[2] Centre de Recherche de Biologie cellulaire de Montpellier (CRBM), University of Montpellier, CNRS, 34293 Montpellier, France.
[3] Centre for Genomic Regulation (CRG), The Barcelona Institute of Science and Technology, Dr Aiguader 88, 08003 Barcelona, Spain.
[4] Universitat Pompeu Fabra (UPF), 08003 Barcelona, Spain.
[5] Institut Catalá de Recerca i Estudis Avançats (ICREA), Pg. Lluís Companys 23, 08010 Barcelona, Spain.
[6] Department of Molecular Biology, Medical Biochemistry and Pathology, Laval University Cancer Research Center, Québec City, QC, G1V 0A6, Canada.
[7] CHU de Québec Research Center, CHUL Pavilion, Oncology Division, Québec City, QC, G1V 4G2, Canada.
[8] RNA Biology Laboratory, Center for Cancer Research (CCR), National Cancer Institute (NCI), National Institutes of Health (NIH), Frederick, MD 21702, USA.

* To whom correspondence should be addressed. Tel: +1-301-846-6816; Email: arunprasath.damodaran@nih.gov; dlarun88@gmail.com
Correspondence may also be addressed to Claude Prigent. Tel: +33(0)434359577; Email: claude.prigent@crbm.cnrs.fr, Erwan Watrin. Tel: +33(0)223234332; Email: erwan.watrin@univ-rennes1.fr and Thomas Gonatopoulos-Pournatzis. Tel: +1-301-846-6095; Email: thomas.gonatopoulos@nih.gov

† The authors wish to be known that, in their opinion, the last three authors should be regarded as Joint Last Authors.

ABSTRACT

The cell cycle regulator Aurora-A kinase presents an attractive target for cancer therapies, though its inhibition is also associated with toxic side effects. To gain a more nuanced understanding of Aurora-A function, we applied shotgun proteomics to identify 407 specific protein partners, including several splicing factors. Supporting a role in alternative splicing, we found that Aurora-A localizes to nuclear speckles, the storehouse of splicing proteins. Aurora-A interacts with and phosphorylates splicing factors both *in vitro* and *in vivo,* suggesting that it regulates alternative splicing by modulating the activity of these splicing factors. Consistently, Aurora-A inhibition significantly impacts the alternative splicing of 505 genes, with RNA motif analysis revealing an enrichment for Aurora-A interacting splicing factors. Additionally, we observed a significant positive correlation between the splicing events regulated by Aurora-A and those modulated by its interacting splicing factors. An interesting example is represented by CLK1 exon 4, which appears to be regulated by Aurora-A through SRSF3. Collectively, our findings highlight a broad role of Aurora-A in the regulation of alternative splicing.

INTRODUCTION

The Aurora kinases are serine/threonine kinases with three members (Aurora-A, Aurora-B and Aurora-C) in mammals (1). The first member of the family was identified in yeast, which has only one Aurora kinase encoded by the gene *Ipl1*, shown to play a role in ploidy regulation (2, 3). Aurora-A was later identified as a protein kinase that localizes to centrosome, is overexpressed in cancers, and is required for bipolar spindle assembly during mitosis (4–6). The level of Aurora-A remains very low during G1 phase and starts to increase in S phase to reach its maximum protein levels at mitosis (7, 8). Aurora-A regulates mitotic spindle assembly, and multiple cell cycle-related events such as centrosome maturation, mitotic entry, cytokinesis and mitotic exit. Thereby, Aurora-A enables proper cell division in coordination with additional cell cycle-regulating proteins (9).

While its role in cell cycle control through phosphorylation of mitotic proteins is well established, recent studies have unveiled novel roles beyond cell cycle regulation such as mitochondrial dynamics, gene regulation and translation (10–12). A high-throughput genetic screen has identified Aurora-A's involvement in apoptosis by affecting RNA splicing. RNA splicing is a crucial step in eukaryotic gene expression, involving the removal of introns and the ligation of flanking exons to form mature mRNA (13, 14). This process is mediated by the spliceosome, a complex and dynamic machinery comprising over 200 proteins (15–19). Splicing is tightly regulated, with complex alternative splicing programs varying across different cell and tissue types, in response to environmental cues, or during cell cycle progression (20, 21). Notably, a significant proportion of alternative splicing events influence key cellular phenotypes, including cell fitness and proliferation (22). While it is well established that RNA-binding protein families, such as SR (serine and arginine-rich) proteins and hnRNPs (heterogeneous nuclear ribonucleoproteins), bind to specific intronic or exonic motifs to modulate splicing (23, 24), the upstream pathways governing the activity of these splicing regulators are less understood.

To ensure programmatic progression of mitosis, normal cells must regulate Aurora-A levels tightly. In contrast, multiple epithelial cancer cells acquire the ability to overexpress Aurora A without compromising cell division, including breast, ovarian, gastrointestinal, colorectal, prostate and lung cancers (25, 26). Indeed, Aurora-A has been characterized as an oncogene that induces genetic instability and ultimately tumorigenesis (27). Aurora-A overexpression likely drives cancer development by promoting cell proliferation, cell survival, stemness, and metastasis and by preventing apoptosis (8). This variety of properties of Aurora-A in tumor development and progression has made it a prime target for the development of cancer therapies. Although many drugs inhibiting Aurora-A kinase have entered clinical development, all have failed in phase III clinical trials due to toxicity (28). Therefore, acquiring a more complete understanding of all Aurora-A functions could potentially identify more precise targeting strategies with less toxic side effects.

To achieve our goal of gaining deeper insights into the full spectrum of Aurora-A functions, we performed a mass spectrometry-based study of the Aurora-A interactome. In the present study, we identified ~400 proteins that specifically associated with Aurora-A. These included known factors required to orchestrate cell division, but also, and more unexpectedly, several mRNA splicing factors that regulate alternative splicing. In a series of functional experiments, we validate that splicing factors

are novel Aurora-A interactors and substrates. Transcriptome profiling analyses reveal that Aurora-A regulates over 600 alternative splicing events, establishing a functional link between Aurora-A and key splicing regulators. Notably, many of these splicing events are also cell cycle-dependent. This study thus uncovers a previously overlooked connection between Aurora-A and cell cycle progression through the regulation of alternative splicing.

RESULTS

Shotgun proteomics analysis of the Aurora-A interaction network uncovers links to RNA splicing

To discover novel interacting partners of Aurora-A, we conducted shotgun proteomics and subsequently performed a comprehensive analysis of proteins identified through Aurora-A affinity purification (**Figure 1A**). As a cell model, we engineered the previously established bone osteosarcoma U2OS cell line, which expresses a GFP-tagged version of Aurora-A under the control of its own promoter (29), to express an shRNA that silences the expression of endogenous Aurora-A mRNA (**Figure 1B**). In this cell line, decreased levels of endogenous Aurora-A leads to an increase in levels of exogenous GFP-Aurora-A protein levels (**Figure 1B**) (29), possibly through compensatory mechanism. We validated that GFP-Aurora-A localized to the interphase centrosome and mitotic spindle (**Supplementary Figure S1A**) and that cell cycle profile was identical to that of wild-type U2OS cells (**Supplementary Figure S1B**) ruling out any abnormal phenotype in the engineered cell line.

To identify Aurora-A-specific interactors, we used wildtype U2OS cells and U2OS cells expressing GFP as negative controls (details in the Methods section). Since the expression of Aurora-A protein level peaks at mitosis, we used paclitaxel (taxol) to synchronize all three cell lines in mitosis and capture a maximum number of interacting partners. We performed affinity-purification using an anti-GFP monoclonal antibody coupled to Protein-G-coated magnetic beads (**Figure 1C**) and validated the presence of active GFP-Aurora-A by western blot analyses using anti-Aurora-A, anti-pT288-Aurora-A and anti-GFP antibodies (**Figure 1D**). We then used liquid chromatography with tandem mass spectrometry to conduct global proteomics analyses (see methods) in which we identified 407 proteins that specifically interacted with Aurora-A (**Figure 1E**). Notably, 36 of the 374 proteins were the previously observed human interactors of Aurora-A as listed in the interaction database BioGRID. (**Figure 1F and Supplementary Table S2**). These interactors included well-characterized Aurora-A effectors such as spindle assemble factor TPX2 (30–32), the centrosomal protein CEP192 (32, 33), cell cycle protein phosphatases PPP6C (34), PPP1CB (35) and the spindle pole associated scaffolding protein WDR62 (36) providing solid indications that our proteomics dataset is likely to contain other relevant interactions. Overall, our large-scale shotgun proteomics analysis of Aurora-A-associated complexes generated a dataset of 371 potential interaction partners or substrates targeted by Aurora-A (**Figure 1F and Supplementary Table S2**).

To explore potential novel functions of Aurora-A, we subjected the interactome data for Gene Ontology (GO) enrichment analysis. This identified several highly significant biological processes (FDR<0.01), including well-known functions of Aurora-A, such as the mitotic cell cycle (4, 5, 9), apoptotic signaling pathway (37, 38), and viral life cycle (39) (**Supplementary Figure S1C**). The enrichment analysis further revealed a few highly enriched biological processes related to mitochondrial functions (**Supplementary Figure S1C-E**), a previously described function of Aurora-A (10, 40, 41). These findings are consistent with the observation derived from analysis using the string-based protein-protein interaction network (**Supplementary Figure S2A**).

Notably, we found that the most enriched terms are linked to RNA-related functions, including mRNA splicing, ribonucleoprotein complex biogenesis (ribosome biogenesis) and regulation of mRNA stability (**Supplementary Figure S1C-E**). By isolating GFP-Aurora-A from cell protein extracts in the presence of nuclease, we minimized the risk of indirectly co-immunoprecipitating proteins through RNA interactions. The string network reveals a subnetwork corresponding to RNA splicing (**Supplementary Figure S2A-B**) whereas the gene enrichment analysis using g:Profiler and DAVID also implicates RNA splicing as a significantly enriched biological process, and with at least 34 proteins corresponding to RNA splicing function (**Supplementary Figure S1D-E**). Although it remains unknown whether Aurora-A directly contributes to the regulation of RNA processing, two previous studies reported that Aurora-A affects RNA splicing by altering the stability of the splicing factor SRSF1 (ASF/SF2) (42, 43). Consistent with this observation, the repertoire of Aurora-A-associated proteins we identified includes several splicing factors, including SRSF1. In addition, a recent study employed BioiD-based proximity labeling, an orthogonal proteomic technique, to identify 440 Aurora-A interactors, including proteins involved in splicing and other RNA processing (44). These converging lines of experimental evidence led us to consider a potential connection between Aurora-A activity and RNA splicing.

To gain further insights into the interaction between Aurora-A and splicing proteins, we capitalized on existing proteomic data of spliceosome subcomplexes (18, 23, 24, 45). In our enrichment analysis (**Supplementary Figure S1D-E**), we found that the Aurora-A interactome shares a significant overlap with known splicing proteins and with more than 16% of previously reported spliceosomal proteins (18, 23, 24, 45) included in the Aurora-A interactome (**Supplementary Figure S3A**). Notably, splicing proteins interacting with Aurora-A are associated with distinct spliceosomal subcomplexes, including early assembly pre-E and E (commitment) complexes, mid-assembly A and B complexes (encompassing components of U2 snRNP and Prp19 complex), and potential components of catalytic C complexes (**Supplementary Figure S3B**). Additionally, a few miscellaneous proteins and the common component of U snRNP (Sm proteins) were also identified (**Supplementary Figure S3B**). Notably, protein subsets involved in the early stages of spliceosome assembly (i.e. pre-E complex, E complex and A complex) were overrepresented (**Supplementary Figure S3B**). Indeed, only 19.5% of Aurora-A-associated splicing proteins corresponded to core spliceosome component responsible for splice site recognition and subsequent conformational changes leading to splicing catalysis (**Supplementary Figure S3B**). In contrast, a vast majority (73.9%) of Aurora-A co-purified splicing proteins belonged to non-core spliceosomal components, which are believed to link the spliceosome to other cellular machineries and functions (24). Remarkably, a substantial proportion (~56%) of these non-core proteins are classified as hnRNP and SR proteins, two types of trans-acting splicing factors known to regulate the spliceosome by either promoting or inhibiting its recruitment at specific splice sites, and thus influencing alternative splicing patterns (46, 47). This enrichment of non-core, regulatory splicing factors in the Aurora-A interactome, suggests that Aurora-A may play a role in modulating alternative splicing.

Aurora-A localizes to nuclear speckles and interacts with splicing factors

Given the interactome of Aurora-A contains multiple splicing factors and these splicing factors are enriched in nuclear speckles, specific intranuclear sites located in the interchromatin region of the nucleoplasm (48), we next investigated whether Aurora-A localizes in nuclear speckles. Upon immunostaining of endogenous Aurora-A and the nuclear speckle marker, SON, we detected by immunofluorescence microscopy that Aurora-A marked a colocalization with SON-stained nuclear speckles (**Figure 2A**). Similarly, we detected colocalization of Aurora-A and another nuclear speckle marker, SRSF2 (SC35) in U2OS cells overexpressing GFP-Aurora-A and U2OS cells stably expressing GFP-Aurora-A, confirming the localization of Aurora-A to nuclear speckles (**Supplementary Figure S4A-C**). These results are strongly supported by a recent proteomic analysis of nuclear speckle proteins (49), further suggesting physical associations between Aurora-A and the splicing machinery.

To validate the interaction between Aurora-A and the splicing factors identified in our proteomic analysis, we conducted co-immunoprecipitation experiments using endogenous proteins. Aurora-A successfully co-purified with all three tested SR proteins, namely SRSF1, SRSF3, and SRSF7 (**Figure 2B**) but not with the negative control, TBP (**Supplementary Figure S4D**). Similarly, we conducted *in vitro* pull-down assays using recombinant Aurora-A and splicing proteins and again demonstrated a direct interaction between Aurora-A and the splicing factors, SR and hnRNP proteins (**Figure 2C-D**). Since splicing factors share well-characterized protein domains that mediate protein-protein or protein-RNA interactions (50), we next asked whether one or more of these domains could mediate direct interactions with Aurora-A. To this end, we used the DAVID tool to search for domains that are enriched in the Aurora-A interactome. In all, we identified a significant enrichment of domains present in splicing factors, particularly the 'RNA recognition motif' domain (RRM), which ranked as the most enriched domain (**Figure 2E and Supplementary Figure S4E**). Altogether, these results demonstrate that splicing factors, likely interact through their RRM domain, are bona fide interactors of Aurora-A. This suggests that Aurora-A may contribute to the regulation of alternative splicing by modulating the functions of these splicing factors.

Inhibition of Aurora-A modulates alternative splicing

To assess the impact of Aurora-A kinase on alternative splicing regulation in human cultured cells, we treated the cells with pharmacological Aurora-A inhibitor and analyzed global changes in alternative splicing. Because perturbation of Aurora-A is well known to delay mitotic entry, prolonging mitosis and inducing mitotic arrest (51–53), we coupled Aurora-A inhibition with cell synchronization (**Supplementary Figure S5A-C**). When assessing synchronization of cells in G1, G2 and mitosis by FACS and determination of mitotic indices, we observed similar cell cycle profiles across control and Aurora-A inhibited cells (**Supplementary Figure S5D-F**). We also confirmed efficient inhibition by immunoblotting using an antibody that recognizes the phosphorylation of Aurora-A at threonine-288 residue, the activation marker of Aurora-A (**Supplementary Figure S5G-I**). These control assays confirm the successful inhibition of Aurora-A and verify that the compared samples consist of cells with similar cell cycle profiles.

To analyze changes in gene expression and alternative splicing caused by Aurora-A inhibition we used edgeR (54) and VAST-TOOLS (21, 55), respectively. Since the inhibitor was applied for 24 hours in our synchronization procedures, where Aurora-A kinase activity remained inhibited in more than one phase of the cell cycle, we considered differentially spliced events as collective Aurora-A hits rather than separating them into G1, G2, or mitotic phase-specific Aurora-A hits (see **Supplementary Figure S5A-C** for synchronization procedures). In total, we identified 622 differentially regulated alternative splicing events in 505 genes upon Aurora-A inhibition (threshold of ΔPSI > 15% or < -15%, **Figure 3A, Supplementary Figure S6A-D and Supplementary Table S3**) while the edgeR tool identified 60 differentially expressed genes (threshold of adjusted P-values of 0.05 and $\log_2$-fold change of 0.5, **Supplementary Table S4**). Only one gene was both differentially spliced and differentially expressed in Aurora-A inhibited condition, suggesting that alternative splicing and gene expression changes represent two separate layers of regulation upon inhibition of Aurora-A. Furthermore, with a cut-off for $\log_2$-fold change of 1.5 and adjusted P-values of 0.05, only one gene (HIST2H2BE) was differentially expressed upon inhibition of Aurora-A (**Supplementary Table S4**). These results strongly indicate that Aurora-A inhibition has marginal effects on gene expression under these experimental conditions. Altogether, our results suggest that the alternative splicing (AS) changes we identified are not a secondary effect of altered transcription but, instead, a direct consequence of Aurora-A inhibition on alternative splicing.

Among the detected changes in alternative splicing (AS) choices, alterations in cassette exons were the most prevalent, accounting for half of the changes (49.7%) (**Figure 3A and Supplementary Figure S6D**). Other common events included alternative 5' splice site (Alt5' SS, 20.4%) and alternative 3' splice site (Alt3' SS, 19.6%). In contrast, intron retention (IR) changes were less common (10.3%) (**Figure 3A and Supplementary Figure S6D**). When comparing the proportion of Aurora-A inhibition-induced alternative splicing event with the total number of alternative splicing events detected, there is no apparent bias towards any particular type of alternative splicing events (**Figure 3A**).

Next, we aimed to determine whether mRNAs for which alternative splicing was affected by Aurora-A inhibition represented particular biological processes. Gene ontology analysis of the 505 affected genes identified enrichment of biological processes such as regulation of transcription, cilium assembly, G2/M transition of the mitotic cell cycle, regulation of autophagy, glucose homeostasis, and positive regulation of GTPase activity (**Figure 3B**). We validated the effect of Aurora-A inhibition in the splicing of key genes involved in these processes such as RCC1, the RAS-related Nuclear Guanine Exchange Factor involved in the mitotic cell cycle, and CELSR3, the protein involved in ciliogenesis (**Figure 3C**) (56, 57). Previous studies have reported roles for Aurora-A in some of these functions (58–60), consistent with the possibility that Aurora-A, at least in part, modulates alternative splicing of the concerned pre-mRNAs to regulate these biological processes.

To explore the functional connection between Aurora-A's splicing function and the cell cycle, we compared splicing event changes between Aurora-A inhibition in HeLa and HEK293T cells with the cell cycle in HeLa cells from our RNA-sequencing data. We observed a significant overlap of splicing events (**Figure 3D**; odds ratio = 6.9; p = 8.8e-86; Fisher's exact test) between Aurora-A inhibition in HeLa cells (**Figure 3A and Supplementary Table S3**) and the cell cycle in HeLa cells (**Supplementary**

Figure S6E and Supplementary Table S5). We also observed a significant overlap of splicing events between Aurora-A inhibition in HEK293T (**Figure 4D and Supplementary Table S6**) and cell cycle-related events in HeLa cells (**Figure 3D**; odds ratio = 1.8; p-value = 0.01; Fisher's exact test), although this overlap was comparatively less significant when compared to the results from Aurora-A inhibition in HeLa cells (**Figure 3D**). This difference in overlap with HeLa and HEK293T is likely due to the use of different cell lines for comparison. However, no significant overlap of splicing events was observed between Aurora-A inhibition in HeLa or HEK293T cells and previously reported cell cycle-related events in HeLa cells (20) (**Supplementary Figure S6F;** HeLa: odds ratio = 0.25; p-value = n.s.; HEK293T: odds ratio = 0.15; p-value = n.s.; Fisher's exact test). One possible reason for the variations could be the number of genes or alternative splicing events initially identified, differences in splicing analysis (tools and reference genome versions used) and thresholds for defining the hits, as has been previously observed in a study to identify periodic gene expression changes (61). Overall, the analysis of our RNA-sequencing dataset suggests that Aurora-A, in addition to its canonical role in mitosis, can partly regulate the cell cycle by impacting alternative splicing.

Functional Interaction Between Aurora-A and Splicing Factors in Alternative Splicing Regulation

Next, we asked if the changes in alternative splicing were due to Aurora-A regulating specific splicing factors with which it interacts. To explore this, we used the Matt tool (62) to identify RNA motifs of splicing factors in pre-mRNA sequences of genes whose splicing is affected by Aurora-A inhibition. Our analysis revealed a significant enrichment of RNA motifs corresponding to several SR and hnRNP proteins (**Figure 4A-C and Supplementary Figure S7-8**). For instance, the RNA motif (M272: RGAAGAAC) corresponding to sequences recognized by SRSF1, was significantly enriched in the upstream intron of upregulated cassette exon events. In contrast, downregulated cassette exon events showed significant enrichment of this motif in both the upstream and downstream introns (**Figure 4A)**. Similarly, for upregulated cassette exons, the RNA motif (M228: HYUUUYU), corresponding to sequences recognized by PTBP1, was significantly enriched in the 3′ region of the upstream intron (**Figure 4B).** This region includes the polypyrimidine tract that is known to mediate the regulatory functions of PTBP1 in some target genes (63). Notably, we observed significant enrichment of RNA motifs of several RRM domain-containing splicing factors such as SRSF1, SRSF2, SRSF7, SRSF9, RALY, PTBP1, HNRNPA1, HNRNPH2, HNRNPA2B1 and HNRNPAB (**Figure 4C**). These observations are consistent with Aurora-A's physical interaction with the RRM domain-containing proteins (**Figure 2C-E and Supplementary Figure S4E**) and suggest a functional interaction between Aurora-A and multiple RRM domain-containing splicing factors.

To explore the functional connections between Aurora-A and SR proteins, we conducted RNA-seq analysis upon knockdown of SRSF1, SRSF2, SRSF3, SRSF7 or inhibition of Aurora-A in HEK293T cells. As a negative control, we also performed RNA-seq analysis upon knockdown of the spicing factor, RBM39, and the core spliceosomal protein, SF3B5, which were not the specific binding partners based on our interactome study (**Supplementary Table S2**). Splicing analysis was subsequently performed using VAST-TOOLS. In total, we identified 2069, 2738, 4245, 1768, 3946 and 11832 differentially regulated alternative splicing events upon knockdown of SRSF1, SRSF2, SRSF3, SRSF7, RBM39 and

SF3B5, respectively (threshold: ΔPSI > 15% or < -15%, **Figure 4D and Supplementary Table S6**). Similarly, we identified 205 differentially regulated alternative splicing events upon inhibition of Aurora-A. Cassette exon was the most prevalent type of splicing event affected by the splicing proteins and Aurora-A (**Figure 4D**). In our comparative analysis, however, we found no obvious difference in the overlap of regulated events between Aurora-A inhibition and the four tested SR proteins or the two negative controls (RBM39 and SF3B5) (**Figure 4E)**. To further investigate the functional connection between Aurora-A and SR proteins, we performed a correlation analysis of the overlapping splicing events. This analysis revealed a significant positive correlation between Aurora-A and the Aurora-A interacting SR proteins: SRSF1 (R = 0.44; p = 0.0395), SRSF2 (R = 0.65; p = 0.0062), SRSF3 (R = 0.51; p = 0.0008) and SRSF7 (R = 0.56; p = 0.012) (**Figure 4E**). However, no significant correlation was observed with the two negative control splicing factors, RBM39 (R = 0.05; p = 0.76) and SF3B5 (R = 0.17; p = 0.45). These findings strongly suggest that Aurora-A interacting splicing factors contribute to the splicing changes affected by Aurora-A inhibition and indicate a functional link between Aurora-A and its interacting splicing factors.

Aurora-A phosphorylates and regulates splicing factors

Considering the crucial role of phosphorylation in regulating the activity of splicing factors to modulate alternative splicing (64–68), we next investigated whether these splicing factors could also serve as substrates for Aurora-A kinase. To address this, we focused on SRSF3, which is a strong binding partner of Aurora-A among the SR proteins, based on our interactome data (**Supplementary Table S2**) and showed a positive correlation with Aurora-A in splicing regulation (**Figure 4E**). Western blot analysis of SRSF3 protein using Phos-tag gels indicated a decrease in the phosphorylation of SRSF3 upon Aurora-A inhibition (**Figure 5A**). Similarly, we observed an increase in SRSF3 phosphorylation upon expression of wildtype but not kinase-dead mutant of Aurora-A, suggesting that SRSF3 is an *in vivo* substrate of Aurora-A (**Figure 5A**). To test if Aurora-A directly phosphorylates SR proteins we performed *in vitro* kinase assays using recombinant SR proteins and Aurora-A. Our kinase assays further revealed that Aurora-A directly phosphorylates SRSF1, SRSF3 and SRSF7 *in vitro* (**Figure 5B-C and Supplementary Figure S9A**). These findings confirm that Aurora-A is capable of phosphorylating several splicing factors and suggest that Aurora-A-mediated phosphorylation could modulate their activity. Since changes in the localization of splicing factors can also alter their function, we carried out an immunofluorescence analysis of SR proteins upon Aurora-A inhibition. However, we did not observe any changes in the localization of these SR proteins upon Aurora-A inhibition (**Supplementary Figure S9B**). Taken together, these findings indicate that Aurora-A mediated phosphorylation of splicing factors could directly regulate their splicing activity rather than altering their localization.

Next, to determine if Aurora-A influences SR-protein activity, we focused on SRSF3, and its known downstream targets, CLK1 poison exon 4 (69). Notably, this exon was also identified as an Aurora-A regulated splicing event by our RNA-seq analysis (**Supplementary Table S3**). First, we confirmed that the splicing of CLK1 exon 4 is dependent on Aurora-A kinase activity through RT-PCR analysis on cells treated with MLN8237 (**Figure 5D**). To further explore if this effect of Aurora-A is

dependent on SRSF3, we knocked down Aurora-A, SRSF3, or both, and subsequently assessed their impact on CLK1 exon 4 splicing (**Figure 5E**). Although knock-down of either Aurora-A or SRSF3 individually leads to increased exon 4 inclusion levels, their combined knock-down does not produce an additive splicing effect. This outcome was observed despite using the same amount of siRNA in each treatment, normalized with non-targeting siRNA sequences (**Figure 5E**). Similar results were observed in both HEK293T and HeLa cells. Furthermore, we observed similar coregulation of the paralogous exon 4 in the *CLK4* gene (70) by Aurora-A and SRSF3 (**Supplementary Figure S9C-D**). These observations suggest that SRSF3 and Aurora-A operate within the same pathway to co-regulate the splicing of exon 4 in both *CLK1* and *CLK4*.

Taken together, our findings suggest that Aurora-A interacts with and phosphorylates splicing regulators, modulating their activity and thereby contributing to the establishment of alternative splicing regulatory programs. Pharmacological inhibition of Aurora-A kinase results in broad alterations in alternative splicing. Collectively, our work sheds light on the broad function of Aurora-A in orchestrating alternative splicing through the regulation of multiple splicing factors.

DISCUSSION

Aurora-A has been identified as a potential drug target in cancer, but all inhibitors developed to date have failed in clinical trials due to adverse effects (28). To realize the therapeutic potential of Aurora-A as an anti-cancer target, it is essential to identify and understand its variety of cellular functions. The Aurora-A interactome we report here revealed novel Aurora-A interactors, suggesting roles in ribosome biogenesis and RNA splicing. Although Aurora-A has not been linked to ribosome biology before, previous studies show that Aurora-A stabilizes SRSF1 and impacts the splicing of genes encoding apoptotic factors (43) and Androgen Receptor (42). Remarkably, our Aurora-A interactome study identified 46 splicing protein interactors, suggesting that Aurora-A interacts with spliceosomal targets beyond SRSF1. A broader role of Aurora-A as a splicing regulator is also consistent with our findings that Aurora-A directly interacts with and phosphorylates multiple splicing factors (hnRNP and SR proteins). Given that hnRNP and SR proteins act as trans-acting splicing factors and affect alternative splicing outcomes (71), we propose that Aurora-A modulates alternative splicing outcomes by interacting with and phosphorylating these splicing factors.

In this study, we showed that Aurora-A interacts predominantly with non-core components of the spliceosome, in particular with members of the hnRNP and SR protein families, regulatory factors of alternative splicing. In related work, Aurora-A was reported to interact with hnRNP proteins such as hnRNPK (11, 72) and hnRNPU (73). Mechanistically, the interaction between Aurora-A and hnRNPK enhanced breast cancer stemness through MYC promoter trans-activation and regulated p53 activity during DNA damage (11, 72) while its interaction with hnRNPU triggered targeting to the mitotic spindle (73). However, the biological significance of these interactions in splicing has not been explored. Our RNA-sequencing analysis revealed changes in alternative splicing events as a consequence of Aurora-A inhibition. Furthermore, our RNA motif analyses revealed the enrichment for sequences bound by Aurora-A-interacting SR and hnRNP proteins, indicating that Aurora-A acts upstream of these splicing factors to influence alterations in alternative splicing. Our study suggests a previously unrecognized functional link between Aurora-A kinase and splicing factors, demonstrated by a significant positive correlation of splicing events regulated by Aurora-A and its interacting SR proteins.

To a lesser extent, Aurora-A also interacts with core spliceosomal proteins such as the RNA helicases (DDX5 and DHX15) and PRP19 complex (PRPF19, BCAS2 and CDC5L). RNA helicases facilitate conformational remodeling between snRNAs at different stages of the splicing reaction (74–77) whereas the PRP19 complex is crucial for activating spliceosome and forming a stable tri-snRNP (78, 79). Consequently, these RNA helicases, PRP19 complex and splicing factors are also implicated in gene regulatory mechanisms such as gene expression, RNA export, RNA degradation, ribosome biogenesis and translation (80–83) and Aurora-A might therefore influence these processes by regulating the DDX5 and DHX15 helicases and the PRP19 complex. This suggests a complex interplay between Aurora-A and gene regulation.

As a critical regulatory mechanism of pre-mRNA splicing, phosphorylation directs numerous components of the splicing process, including spliceosome reorganization, protein-protein interactions, recruitment of splicing factors to the transcription site, catalysis of the splicing reaction, and splicing outcomes (64, 66, 67, 84). Our findings that Aurora-A phosphorylates several SR and hnRNP proteins,

and that its inhibition perturbs alternative splicing, are in agreement with a phospho-proteomics study that identified splicing factors HNRNPA1, HNRNPK and RBMX (present in our interactome) as candidate Aurora-A *in vivo* substrates (85). Similar to Aurora-A, other cell cycle-regulating kinases (AKT, MAPKs, PTKs, NEK2 and PKA) have also been reported to modulate splicing mechanisms (86–91), suggesting that splicing regulation is integrated with other cellular processes in response to physiological and pathological stimuli.

A key future objective is to identify the specific phosphorylation sites responsible for the regulatory effects in the identified splicing factors. In this study, we sought to rescue the effects of SRSF3 depletion by reintroducing siRNA-resistant phospho-mutants at individual sites (S5A, S128A, or S138A), which are among the top predicted phosphorylation sites of SRSF3 by Aurora-A, based on prior research (92). However, no significant differences were observed in the rescue of *CLK1* exon 4 splicing between the wild-type SRSF3 and the tested phospho-mutants (**Supplementary Figure S9E**). It is important to note that these three sites represent only a subset of the eight high-confidence serine residues predicted to be phosphorylated by Aurora-A. This suggests that redundancy among phosphorylated residues may mask the effects of individual site mutations. Consequently, inhibiting multiple phosphorylation sites in SRSF3 and other SR proteins might be required to achieve a measurable impact on alternative splicing.

Alternative splicing has been known to be altered during the cell cycle due to the altered expression of splicing factors (20). Although our RNA sequencing data indicate that Aurora-A inhibition does not lead to any changes in the expression of splicing factors in any of the cell cycle stages, the existence of functional and regulatory interactions during the cell cycle cannot be ruled out. For instance, altered expression of splicing factors and Aurora-A and the subsequent change in their interactions during the cell cycle can regulate cell cycle-dependent splicing events. Aurora-A may also regulate alternative splicing post-translationally as observed for SRSF1 (43). Further proteomic and phospho-proteomic studies at different cell cycle stages are needed to gain a deeper understanding of the different modes of splicing regulation by Aurora-A.

Our work shows that inhibiting Aurora-A kinase activity affects the splicing of more than 600 alternative splicing events, with a significant overlap with cell cycle-regulated splicing events (**Figure 3D**) (20). In particular, this affects the alternative splicing of genes involved in cell cycle-related functions such as cilium assembly, GTPase activity, and G2/M transition. As these functions are often misregulated in cancer (93–96), Aurora-A may regulate the cell cycle and help cancer cell growth by modulating alternative splicing alongside its established cell cycle functions (97). In agreement with this, two previous studies (42, 43) reported the alteration in the splicing of apoptotic genes during mitotic arrest and the AR gene in prostate cancer. Although we here identified cell cycle-related splicing events as Aurora-A hits, the biological consequences of these events on cell cycle regulation and cancer progression await further investigations. With the advent of CRISPR-based exon perturbation technologies for genome-scale screens (22, 98–101), the effect of these splicing events on the cell cycle and cancer progression can be evaluated in a high throughput manner when these screening technologies are coupled with cell cycle-based reporter and proliferation-based phenotypic assays. Recent studies have deepened our insight into distinct functions of Aurora-A (102–104). Specifically,

the application of “PROTACS” to study cell biology at spatial resolution has advanced our understanding of processes regulated by Aurora-A in distinct sub-cellular compartments (103, 104). These advances, along with our work, bring fresh perspectives of Aurora-A functions and how these can be more specifically harnessed to target cancer cells while avoiding toxic side effects.

MATERIALS AND METHODS

Expression vectors and molecular cloning

The plasmid constructs were generated using Gibson Assembly Master Mix (New England Biolabs). The cDNAs of splicing proteins were PCR amplified and subcloned into pGEX4T1 vector. The cDNA of Aurora-A was PCR amplified and subcloned into pDONR223 destination vector using BP clonase II (Thermo Fisher Scientific) and subsequently to pcDNA5-3xFLAG vector using LR clonase II (Thermo Fisher Scientific). All plasmid constructs were verified by sequencing. All the pCS2+ FLAG-tagged SRSF constructs for expression in mammalian cells were a kind gift from Dr. Wei Wu (105). All the GST tagged SRSF constructs for expression in bacterial cells were a kind gift from Dr. Evelyne Manet (106). The kinase-dead mutant (T287A, T288A) of pcDNA5-3xFLAG-tagged Aurora-A construct was generated using Q5® Site-Directed Mutagenesis Kit (New England Biolabs). The primer sequences are given in **Supplementary Table S1**.

Cell culture and transfection

U2OS, HEK293T and HeLa cells were grown in Dulbecco's modified Eagle's medium (DMEM)-GlutaMAX™ -I (Sigma-Aldrich) supplemented with 10% fetal bovine serum (GE Healthcare) and 1% penicillin–streptomycin (GE Healthcare). For transfection experiments, cells were grown until they reached 60% confluency and the plasmids and siRNAs (Dharmacon; 25nM) were transfected using Lipofectamine-3000 and Lipofectamine™ RNAiMAX (Thermo Fisher scientific) transfection reagents respectively according to the manufacturer's instructions. The siSRSF3-3'UTR (107) (5'-GAAGUGGUGUACAGGAAAU-3'; Dharmacon; 25nM) was used for the knockdown of endogenous SRSF3 and rescue with wildtype or phospho-mutants of SRSF3, whereas, non-targeting siRNA (siNT) was used as a control.

Cell synchronization and inhibition of Aurora-A

For synchronization of HeLa cells at G1 phase, we used a double thymidine block method where Aurora-A inhibitor (MLN8237) was added immediately after the first thymidine release when the cells were in G1 phase. Then, non-mitotic cells were collected after 24 hours of Aurora-A inhibitor (50 nM) treatment. For synchronization at G2 phase, we released cells for 6 hours from double thymidine block. Aurora-A inhibitor was added 6 hours after the first thymidine release when the cells were in G2 phase. Then, non-mitotic cells were collected after 24 hours of Aurora-A inhibitor treatment. For synchronization at mitotic phase, we released cells for 12 hours from double thymidine block. Aurora-A inhibitor was added 12 hours after the first thymidine release when the cells were in late G2 or mitotic phase. Then, mitotic cells were collected after 24 hours of Aurora-A inhibition. Nocodazole (3.3 μM) was added two hours prior to harvesting cells to collect a maximum number of mitotic cells.

Generation of U2OS-GFP-Aurora-A with shRNA-Aurora-A stable cell line

Stable depletion of endogenous Aurora-A in U2OS-GFP-Aurora-A cell line (29) was obtained by the transfection of shRNA directed against the 3' UTR region of Aurora-A (clone NM_003600.x-

985s1c1, Sigma) followed by clonal dilution and selection of Aurora-A depleted cells with 2 μg/ml of puromycin.

Western blot analysis

The cells were washed with PBS twice and scraped directly in 2X Laemmli sample buffer and boiled at 95°C for 5 minutes. The protein concentration was quantified using the Protein Quantification Assay kit (Macherey-Nagel). The protein samples were resolved using 4–15% Mini-PROTEAN™ TGX Stain-Free™ Protein Gels (Bio-Rad) and transferred onto PVDF membrane (GE Healthcare) and analyzed by western blotting. The following primary antibodies were used: rat anti-α-tubulin (MAB1864, Millipore, 1:10000), mouse anti-Aurora-A (clone 5C3, 1:100 (108)), rabbit anti-phospho-Aurora-A/B/C (clone D13A11, 2914, Cell Signaling Technology, 1:500), mouse anti-ASF/SF2 (clone 96, 32-4500, Thermo Fisher Scientific, 1:10000), mouse anti-GST tag (G1160, Sigma 1:2000), mouse anti-His tag (HIS.H8 / EH158, Covalab, 1:2500), mouse anti-FLAG tag (clone M2- F1804, Sigma, 1:1000), mouse anti-GFP (clones 7.1 and 13.1, Roche Applied Science, Indianapolis, IN, 1:1000). Corresponding secondary horseradish peroxidase-conjugated antibodies were used: anti-mouse and anti-rabbit (Jackson Immuno Research Laboratories) and anti-rat (A110-105P, Bethyl Laboratories). Membranes were incubated with a lab-made enhanced chemiluminescence reagent containing 100 mM Tris (pH 8.5), 13 mg/ml coumaric acid (Sigma), 44 mg/ml luminol (Sigma) and 3% hydrogen peroxide (Sigma). Chemiluminescence signals were captured on a film (CP-BU new, Agfa Healthcare) with a CURIX 60 developer (Agfa Healthcare).

Affinity-purification of Aurora-A-interacting proteins

Multiple biological and technical replicates were used to generate a highly specific dataset of Aurora-A-associated proteins. Experiments were performed in triplicates and injected in two fractions for LC-MS/MS analysis (a total of 6 replicates for control experiments and 12 replicates corresponding to GFP-Aurora-A affinity-purification extracts). To assess the non-specific binding to our affinity-purification matrix (i.e. Dynabeads coupled to anti-GFP antibodies), whole cell extracts of wild-type human osteosarcoma U2OS cells and U2OS cells expressing GFP were used. For affinity-purification of Aurora-A-associated protein complexes, whole cell extracts of U2OS cells stably expressing a GFP-tagged version of human Aurora-A were used. Wild-type and GFP-Aurora-A expressing U2OS cells were seeded onto three 150 mm cell culture dishes and grown up to 75% confluency. Cells were incubated with 1 μg/ml paclitaxel for 18 h to cause a mitotic arrest. Two PBS washes were carried out prior to harvesting the cells with disposable cells scraper. All the affinity-purification steps were carried out at 4°C unless mentioned otherwise. Three mL/plate of lysis buffer (50 mM HEPES pH 7.5, 150 mM NaCl, 0.3% CHAPS and supplemented with cOmplete™ EDTA-free protease inhibitor cocktail (Roche) and 100 units mL Benzonase® nuclease (Sigma-Millipore)) were used during cells scraping. Cells were kept on ice and lysed for 30 min on a rotating device. Cell extracts were centrifuged for 5 min at 10,000 rpm to remove cellular debris. Immunoprecipitation experiments were performed using Dynabeads™ magnetic beads covalently coupled with Protein G (Life Technologies). The Dynabeads™ were washed once with 2 ml of PBS and coated with 15 μg of mouse monoclonal anti-GFP antibody (Roche Applied

Science). The beads were finally washed three times with 2 ml of lysis buffer and added to the whole cell extract for a 2 h incubation with gentle rotation. Samples were then washed three times with 1 volume of lysis buffer for 10 min. Beads were resuspended in a 75 mM ammonium bicarbonate solution (pH 8.0) and protein complexes were directly digested on-beads by the addition of 2 μg of a Trypsin/Lys-C mixture (Promega). Peptides were isolated on C18 resin tips according to the manufacturer's instructions (Thermo Fisher Scientific) and dried to completion in a speed vac evaporator.

Liquid-chromatography tandem mass spectrometry (LC-MS/MS)

All samples were processed on an Orbitrap™ Fusion™ Tribrid™ mass spectrometer (Thermo Fisher Scientific). Peptide samples were separated by online reversed-phase (RP) nanoscale capillary liquid chromatography (nanoLC) and analyzed by electrospray mass spectrometry (ESI MS/MS). The experiments were performed with a Dionex UltiMate 3000 nanoRSLC chromatography system (Thermo Fisher Scientific / Dionex Softron GmbH, Germering, Germany) connected to the mass spectrometer equipped with a nanoelectrospray ion source. Peptides were trapped at 20 μl/min in loading solvent (2% acetonitrile, 0.05% TFA) on a 5 mm x 300 μm C18 pepmap cartridge pre-column (Thermo Fisher Scientific / Dionex Softron GmbH, Germering, Germany) for 5 minutes. Then, the pre-column was switched online with a self-made 50 cm x 75μm internal diameter separation column packed with ReproSil-Pur C18-AQ 3 μm resin (Dr. Maisch HPLC GmbH, Ammerbuch-Entringen, Germany) and the peptides were eluted with a linear gradient from 5-40% solvent B (A: 0,1% formic acid, B: 80% acetonitrile, 0.1% formic acid) in 60 minutes, at 300 nL/min. Mass spectra were acquired using a data dependent acquisition mode using Thermo XCalibur software version 3.0.63. Full scan mass spectra (350 to 1800m/z) were acquired in the orbitrap using an AGC target of 4e5, a maximum injection time of 50 ms and a resolution of 120 000. Internal calibration using lock mass on the m/z 445.12003 siloxane ion was used. Each MS scan was followed by the acquisition of fragmentation spectra of the most intense ions for a total cycle time of 3 seconds (top speed mode). The selected ions were isolated using the quadrupole analyzer in a window of 1.6 m/z and fragmented by Higher energy Collision-induced Dissociation (HCD) with 35% of collision energy. The resulting fragments were detected by the linear ion trap in rapid scan rate with an AGC target of 1e4 and a maximum injection time of 50 ms. Dynamic exclusion of previously fragmented peptides was set for a period of 20 sec and a tolerance of 10 ppm.

Processing of mass spectrometry data

Mass spectra data generated by the Orbitrap™ Fusion™ Tribrid™ instrument (*.raw files) were analyzed by MaxQuant (version 1.5.2.8) using default settings for an Orbitrap instrument. Andromeda was used to search the MS/MS data against FASTA-formatted Homo sapiens Uniprot Reference Proteome UP000005640 (70 611 entries) complemented with GFP-Aurora-A amino acid sequence and a list of common contaminants maintained by MaxQuant and concatenated with the reversed version of all sequences (decoy mode). The minimum peptide length was set to 7 amino acids and trypsin was specified as the protease allowing up to two missed cleavages. The false discovery rate (FDR) for peptide spectrum matches (PSMs) was set at 0.01. The following mass additions were used as variable modifications: oxidation of methionine [+15.99491 Da], deamidation of asparagine and glutamine

[+0.98401 Da], N-terminal acetylation [+42.01056 Da] and phosphorylation of serine and threonine [+97.97689 Da]. MaxQuant output files were imported in Scaffold (version 4.6.1, Proteome Software Inc) to validate MS/MS based peptide and protein identifications. Peptide and protein identifications were accepted if they could be established at greater than 95% probability to achieve an FDR less than 1%. Common contaminants (i.e. keratins, serum albumin, IgGs, trypsin, ribosomal subunit proteins, etc) were removed from the output file. Proteins found as non-specific binders of magnetic beads coupled to anti-GFP antibodies were removed from the GFP-Aurora-A-specific dataset unless they are assigned with 10 times more peptide spectrum matches (PSMs).

Finally stringent cut-off was applied to obtain the specific interactors of Aurora-A where the proteins with sequence coverage less than 5%, Label free quantification (LFQ) for control not equal to 0 and LFQ for Aurora-A equal to 0 were filtered out.

Gene ontology enrichment analysis

The Gene Ontology enrichment analysis was carried out using the tool g:Profiler (109) using the GO biological processes and following parameters (Significance threshold - Benjamini and Hochberg method; User threshold: 0.05; minimum term size is 5 and maximum term size is 350). The functional GO terms were visualized using Enrichment Map plugin v3.3.0 (110) available in the Cytoscape v3.8.0 (111) with following parameters (FDR q-value cutoff of 0.01; p-value cutoff of 0.001; metric: overlap; metric cutoff: 0.8). The redundant functional GO terms were arranged and grouped (mcl clustering) based on similarity using AutoAnnotate plugin v1.3.3 (112) available in the Cytoscape v3.8.0. In enrichment maps, node size is proportional to the gene-set size, border width colour is proportional to FDR (q-value) and edge width is proportional to the number of genes shared between GO categories. Alternately, gene ontology enrichment analysis was carried out using the DAVID tool (113, 114). For all GO enrichment analysis, the default background (human proteome) as assigned by the tools was used.

Construction of protein-protein interaction network

The protein-protein network was constructed using Cytoscape v3.8.0 and the integrated network query using STRING plugin v1.5.1 (115) with the Confidence (score) cutoff of 0.9 and maximum additional interactors of 0. The sub-networks or clusters were visualized using mcode plugin v1.6.1 (116) available with Cytoscape v3.8.0.

Co-Immunoprecipitation

HeLa cells synchronized at mitosis were washed with PBS and lysed in F buffer (10 mM Tris pH 7.05, 50 mM NaCl, 30 mM Na_4 pyrophosphate, 50 mM NaF, 5 µM $ZnCl_2$, 10% glycerol, 0.5% Triton X-100) supplemented with a protease inhibitor cocktail (Roche #11836170001) and 150 units/ml of Benzonase Nuclease (E1014, Sigma). The lysates were centrifuged at 18,500 rcf for 10 minutes at 4°C to collect the supernatant. 2ug of total cell lysates were incubated with Dynabeads protein G (ThermoFisher Scientific #10004D) bound to 2ug of specific antibodies against SRSF1 (Proteintech, #12929-2-AP), SRSF3 (MBL, #RN080PW), SRSF7 (Proteintech, #11044-1-AP), TBP (Proteintech,

22006-1-AP) or Rabbit IgG (Proteintech, #30000-0-AP) overnight at 4°C with rotation. The beads were washed 3 times using F buffer, and bound protein complexes were eluted by boiling in NuPAGE LDS Sample Buffer (ThermoFisher Scientific # NP0007) at 70°C for 10 minutes. The eluted proteins were then subjected to western blot analysis using specific antibodies against SRSF1, SRSF3, SRSF7, TBP, TAF5 (Thermo Fisher Scientific, #MA3-076) and Aurora-A.

Expression and purification of recombinant proteins

E.coli strain BL21 (DE3) was transformed with GST fusion plasmids encoding HNRNPC, RALY, PCBP2, PTBP1, RS26, eIF4A3, SRSF1, SRSF3 and SRSF7 or HIS fusion plasmid encoding Aurora-A. Cells were grown till the OD600 reached 0.6 in 250 ml LB media supplemented with antibiotics (ampicillin 100 μg/ml or kanamycin 50 μg/ml) and expression of the protein was induced for 4 hours with 1 mM isopropyl 1-thio-B-D-galactopyranoside (Sigma) at 18°C. Cells were collected and sedimented by centrifugation for 20 min at 4000 rpm (4°C). The cell pellet for HIS-tagged protein purification was resuspended in 10 ml of Buffer A (20 mM Tris pH 7.5, 500 mM NaCl, 20 mM imidazole) containing 1X protease inhibitors (EDTA free protease inhibitor cocktail, Roche). Whereas for purification of GST tagged proteins, cell pellets were resuspended in 10 ml of Buffer B (0.1% Triton X100 in PBS) supplemented with 1X protease inhibitors. The cells were then sonicated at 50% amplitude for 3 min (30 sec pulses) and cell lysates were centrifuged at 10000 rpm for 30 min at 4°C. The supernatant was incubated with TALON His-tag purification resin (TaKaRa) or glutathione agarose beads (Sigma-Aldrich) for 30 min in a rocker at 4°C. Beads were then washed thrice with buffer and eluted with 250 mM imidazole (for HIS-tagged proteins) or 5 mM reduced glutathione (for GST-tagged proteins). Protein profiles from the eluted fractions were estimated by SDS-PAGE followed by Coomassie staining.

***In vitro* interaction assay**

For GST pull-down assays, the GST-tagged hnRNP and HIS-tagged Aurora-A were incubated in interaction buffer (containing 50 mM Tris-HCl, pH 7.5, 100 mM KCl, 10 mM $MgCl_2$, 5% glycerol, 1 mM DTT and 0.25% NP40) for 2 hours in a rocker at 4°C and the complex was pulled down using Glutathione Sepharose 4B beads. The interaction of splicing proteins with Aurora-A was analyzed by western blots against anti-GST and anti-HIS or anti-Aurora-A antibodies.

For FLAG pull-down assays, FLAG-tagged SR proteins (SRSF) were expressed in HEK293T cells and the cells were lysed with M2 lysis buffer (50 mM Tris-base (pH 7.4), 150 mM NaCl, 10% glycerol, 1% Triton X-100 and 1 mM EDTA). The FLAG-tagged SR proteins were incubated with FLAG-M2 beads and were washed thrice with M2 lysis buffer. The bound FLAG-tagged SR proteins were incubated with recombinant HIS-tagged Aurora-A for 2 hours in a rocker at 4°C. The beads containing protein complexes were again washed thrice and eluted with 100 μg/ml of FLAG peptide. The interaction of SR proteins with Aurora-A was analyzed by western blots against anti-FLAG and anti-HIS or anti-Aurora-A antibodies.

Phos-tag Gel Electrophoresis

HeLa cells were lysed in F buffer supplemented with a protease inhibitor cocktail (11836170001, Roche) and PhosSTOP™ (4906845001, Roche). The lysates were centrifuged at 18,500 rcf for 10 minutes at 4°C to collect the supernatant. 30 µg of cell lysate was mixed with Laemmli Sample Buffer (Bio-Rad #1610747) and separated using 12.5% SuperSep™ Phos-tag™ gels (50 µM, FujiFilm Wako, 199-18011). Following electrophoresis, the gel was washed three times in transfer buffer containing 1 mM EDTA for 20 minutes each to remove Zn2+ ions, then washed in transfer buffer without EDTA. Proteins were transferred to an Immobilon-P PVDF membrane (Millipore #IPVH00010) at 100 V for 120 minutes using the Mini Trans-Blot® Module (Bio-Rad #1658030) in a wet transfer setup and subjected to western analysis using an SRSF3 antibody.

***In vitro* kinase assay**

Recombinant GST-tagged splicing proteins and HIS-tagged Aurora-A were incubated in kinase buffer (containing 50 mM Tris-HCl, pH 7.5, 50 mM NaCl, 1 mM DTT, 10 mM $MgCl_2$ and 100 µM ATP) in presence of [γ-^{32}P]-ATP at 37°C for 30 minutes. The reaction was stopped by the addition of 2X Laemmli sample buffer and boiled at 95°C for 5 min. Phosphorylated splicing proteins were resolved by SDS-PAGE on 10% gels and visualized by autoradiography.

Immunofluorescence staining and microscopy

Cells grown on coverslips were fixed with methanol (−20°C) for 5 minutes. The cells were then blocked with 5% FBS in PBS and incubated with SRSF2 (SC35) (Sigma, #S4045, 1:2000 or Proteintech, #20371-1-AP, 1:200), SRSF1 (Proteintech, #12929-2-AP, 1:200), SRSF3 (MBL, #RN080PW, 1:100) primary antibodies in blocking solution for 1 hour at room temperature. Cells were washed thrice in PBS containing 0.05% Tween 20 and incubated with secondary antibody (anti-mouse or anti-rabbit antibody conjugated to Alexa Fluor 488 or 546 or 647 (Thermo Fisher Scientific) at 1:4000 dilutions and GFP nano-booster (Chromotek) at 1:1000 dilution in blocking solution for one hour at room temperature. The cells were then washed and the DNA was stained using Hoechst 33342 (Thermo Fisher Scientific) or DAPI. Finally, the coverslips were mounted using ProLong® Gold antifade reagent (Thermo Fisher Scientific) or Fluoromount-G Mounting Medium (ThermoFisher Scientific). High-resolution images were taken with the LSM800 Airyscan confocal microscope (Zeiss Inc.) equipped with 63X/1.4 Plan Apochromat Oil DIC objective and Airyscan detector (airyscan mode). The images were processed with FIJI (ImageJ) software.

For live cell imaging, stable U2OS cells expressing GFP-Aurora-A and shRNA-Aurora-A were grown in 35 mm glass-bottomed dishes (Matek Corporation) Z-sweeps of 0.3 µm sections were acquired for both GFP and DAPI channels. Subsequent analysis was carried out using Fiji (ImageJ) software.

Flow cytometry analysis and mitotic index calculation

After the cell cycle specific synchronization, HeLa cells were washed twice with PBS and was resuspended in 70% ice-cold methanol and incubated at 4°C for 1 hour. Pellets were washed twice with PBS and resuspended in PI buffer containing 50 µg/ml propidium iodide, 10 mM Tris pH7.5, 5 mM

$MgCl_2$, 200 μg/ml RNase A and incubated at 37°C for 30 minutes. The percentage of cells in each cell cycle phase was calculated with a Fortessa X-20 LSR (Becton Dickinson). The mitotic index of FACS samples was calculated in order to discriminate the cells in G2 and mitotic phase. The samples prepared for FACS analysis were mounted on a glass slide and counted using a fluorescence microscope (DMRXA2 Leica). At least 100 cells were counted for each condition.

RNA-sequencing analysis

Total RNA was isolated from two replicates of the synchronized HeLa cells using the RNeasy Plus Mini Kit (QIAGEN) as per the manufacturer's protocol. While isolating total RNA for RNA-seq analysis, on-column digestion of DNA was additionally performed using RNase-Free DNase Set (QIAGEN) as a precautionary measure. The mRNA-seq libraries were sequenced using 125bp paired-end reads on Illumina HiSeq 2500 lanes. The library preparation and sequencing were performed in the CRG Genomics Unit. The quality of the RNA sequencing data was evaluated using the MultiQC tool. The reads were aligned using the Star alignment program to the hg38 human reference genome. The read counts were corrected using edgeR upper quartile normalization factors. Differential gene expression analysis between Aurora-A inhibited and control conditions were carried out using edgeR tool (54) and a final cut-off for log_2-fold change of 0.5 and adjusted P-value of 0.05 were applied. Alternative splicing analysis was carried out using *vast-tools* v2.2.0 pipeline (21, 55) which is available in github (https://github.com/vastgroup/vast-tools). PSI values for two replicates were quantified for all types of events (cassette exons, alternative 3′ and 5′ splice sites and retained introns). A minimum ΔPSI of 15% was required to define differentially spliced events with a minimum range of 5% between the PSI values of the two samples (control and Aurora-A inhibited samples). Similarly, cell cycle-regulated splicing events were identified by comparing the control samples of each cell cycle stage (G1 vs G2, G2 vs M, M vs G1). The RNA motif enrichment for splicing factors/RBP were carried out using *Matt-tool* v1.3.0 (62) with the differentially spliced events ($|\Delta PSI| > 15$) and unregulated splicing events as inputs for computing the enrichment profile.

Similarly, the RNA sequencing and splicing analysis for HEK293T samples were performed c at the CCR Sequencing Facility. The mRNA-seq libraries were subjected to paired-end sequencing using an Illumina NovaSeq_X_Plus_10B platform with a 200-cycle kit. On average, the SRSF1, SRSF2 and SRSF7 samples have 114 million pass filter reads, with more than 94% of bases above the quality score of Q30. On average, the SRSF3, Aurora-A inhibition and Aurora-A knockdown samples have 219 million pass filter reads, with more than 95% of bases above the quality score of Q30. The splicing analysis was performed as mentioned above.

Splicing analysis using one-step RT-PCR

HeLa and HEK293T cells were treated with 2 μM MLN8237 or transfected with 25 nM siRNA (Dharmacon) targeting Aurora-A or SRSF3 using Lipofectamine RNAiMAX (Thermo Fisher Scientific) for 72 hours. Total RNA was extracted using RNeasy Plus Kit (QIAGEN) and the splicing pattern was then monitored by one-step RT-PCR analysis (Qiagen). The RT-PCR products were separated on 2% agarose gels and quantified using FIJI software.

DATA AVAILABILITY

The mass spectrometry proteomics data of Aurora-A have been deposited to the ProteomeXchange Consortium (117) via the PRIDE (118) partner repository with the dataset identifier PXD021093.

RNA-sequencing data generated from this study have been deposited in Gene Expression Omnibus (119) under the accession number GSE160733.

ACKNOWLEDGEMENTS

We are grateful to Stephanie Dutertre of the Microscopy-Rennes Imaging Center (Biologie, Santé, Innovation Technologique, BIOSIT, Rennes, France). We thank Kanchana Nandanan Chathoth (CIMIAD, U1241 NUMECAN, Rennes, France) for proofreading the article.

FUNDING

Work by C.P.'s team is supported by the University of Rennes 1, the CNRS, and the Ligue Nationale Contre le Cancer “Équipe labellisée 2014-2017” and ligue35. The PhD salary of A.P.D. and the post-doc salary of T.C are supported by the Ligue Nationale Contre le Cancer and the Bretagne region. This work is also supported by the NCI/NIH Intramural Research Program (Project ZIABC012019). Work in J.V. lab was supported by Spanish Ministry of Science and Innovation, EMBL Partnership and Severo Ochoa Centre of Excellence. We also acknowledge the support of CRG core facilities.

CONFLICT OF INTEREST STATEMENT

The authors declare no conflict of interest.

FIGURES LEGENDS

Figure 1. Identifying new interacting partners of Aurora-A.

(A) Schematic representation of the strategy used to isolate and identify Aurora-A interacting proteins in human cells. Two negative controls (wild-type U2OS cells and U2OS cells expressing GFP) and U2OS with stable expression of GFP-Aurora-A and shRNA-Aurora-A were used. Cells were synchronized in mitosis by overnight incubation with Taxol. GFP and GFP-Aurora-A were isolated by affinity-purification coupled to mass spectrometry (AP-MS). (**B**) Western blot analysis of the expression level of GFP-Aurora-A. Protein extracts prepared from control U2OS cells (1), from cells expressing GFP-Aurora-A (2), and from cells expressing GFP-Aurora-A and Aurora-A-shRNA (3) were analyzed by western blot. Endogenous Aurora-A and GFP-Aurora-A protein were detected by anti-Aurora-A antibody (top panel) while the activated kinase by anti-phospho-Thr288 (middle panel). Actin was used as a loading control (lower panel). (**C**) Sypro Ruby gel staining of proteins co-pulled down by anti-GFP antibody from control U2OS cells (1) and U2OS cells expressing GFP-Aurora-A and Aurora-A-shRNA (2). (**D**) Western blot analysis of control (1) or affinity-purified GFP-Aurora-A (2) with anti-Aurora-A antibody (top panel), anti-pThr288 antibody (middle panel) and anti-GFP antibody (lower panel). (**E**) Scatter plot shows the relative abundance of proteins (logarithmized Label-free quantification (LFQ) values) in control samples versus Aurora-A affinity-purified samples. The common contaminants and proteins with sequence coverage less than 5% were excluded for this analysis. The red circles indicate the interacting partners specific to Aurora-A. (**F**) The top 100 proteins in the filtered proteomics dataset of 407 Aurora-A specific interacting proteins as visualized in Cytoscape.

Figure 2. Aurora-A localizes to nuclear speckles and directly interacts with splicing factors. (**A**) The top panel shows the immunofluorescence microscopy staining of endogenous Aurora-A (green) and the nuclear speckles marker, SON (red). Scale bar, 5 μm. The bottom panel is the line scan analysis using Fiji with local intensity distributions of Aurora-A and SON. The merged image on the right indicates the position of the line scan with a white line. (**B**) Western blot analysis of total cell lysates (input) and SRSF immunoprecipitates (IPs: SRSF1, SRSF3 and SRSF7) from Hela cells synchronized in mitosis. Immunoglobulin G (IgG) immunoprecipitation was performed as a control. Blots were probed with antibodies specific for SRSF1, SRSF3, SRSF7 and Aurora-A. (**C**) GST pull-down assay showing the direct interaction of the SR proteins with Aurora-A *in vitro*. The bottom panel shows the stain-free gel image of purified recombinant HIS-tagged Aurora-A and GST-tagged SR proteins used for interaction assay. The top panel is the western blot showing the GST pull-down assay between HIS-tagged Aurora-A and GST-tagged SR proteins. GST was used as a negative control. (**D**) GST pull-down assay showing the direct interaction of the hnRNP proteins with Aurora-A *in vitro*. The left panel shows the Coomassie staining of purified recombinant HIS-tagged Aurora-A and GST-tagged hnRNP proteins used for interaction assay. The right panel is the western blot showing the GST pull-down assay between HIS-tagged Aurora-A and GST-tagged hnRNP. GST was used as negative control and NPM was used as a positive control. (**E**) Dot plot summarizing the domain enrichment analysis of Gene Ontology (GO) against the InterPro database using the filtered Aurora-A protein interaction dataset (407 Aurora-A

interacting proteins). The top 10 predominant domain terms were plotted relative to their -$\log_{10}$(P values).

Figure 3. Aurora-A modulates alternative splicing patterns. (A) Bar graph showing the different categories of alternative splicing (AS) events affected by Aurora-A inhibition and the total number of alternative splicing events identified. The y-axis indicates the type of events and the x-axis indicates the number of differentially spliced events. The pie chart within the bar graph shows the distribution (proportion) of alternative splicing event types. CE: Cassette exons, IR: Intron retention, Alt3'ss: alternative 3' splice sites, Alt5'ss: alternative 5' splice sites (**B**) Dot plot showing the top 15 enriched GO term obtained from the analysis of all the differentially spliced events across the cell cycle using the DAVID tool. The plot indicates the significance and the number of gene (protein) counts that are mapped to each GO terms. (**C**) RT-PCR assay monitoring the alternative splicing of genes from HeLa cells treated with MLN8237 for 72 hours. Corresponding Percent Spliced In (PSI) values from three independent experiments are shown as bar plots on the right panel. Two-tailed unpaired t-tests are applied. **(D)** Venn diagram showing overlap of splicing events between Aurora-A inhibition (in HeLa or HEK293T) and cell cycle in HeLa cells (from this study). Fisher's exact test is applied.

Figure 4. Aurora-A modulates alternative splicing through multiple splicing factors. (**A**) Enrichment of RNA motif (M272: RGAAGAAC) of SRSF1 in alternative splicing events affected by Aurora-A inhibition during mitosis. The blue, brown and grey lines show the enrichment for motif on upregulated (ΔPSI > 15%), downregulated (ΔPSI < -15%) and unregulated splicing events respectively. Regions with thick lines indicate the significant enrichment (FDR ≤0.05, 1000 permutation). (**B**) Enrichment of RNA motif (M228: HYUUUYU) of PTBP1 in alternative splicing events affected by Aurora-A inhibition in G2 phase. (**C**) Table summarizing the RNA motif enrichments of the SR and hnRNP proteins. (**D**) Bar graph showing the different categories of alternative splicing (AS) events affected by Aurora-A inhibition and splicing factor knockdowns. The pie chart within the bar graph shows the distribution (proportion) of alternative splicing event types. (**E**) Venn diagram showing overlap of splicing events between Aurora-A inhibition (MLN8237) and splicing factor knockdowns (SRSF1, SRSF2, SRSF3, SRSF7, RBM39 and SF3B5) in HEK293T cells. On the right panel are the plots showing the correlation of ΔPSI values of the overlapping splicing events. P values less than 0.05 are considered non-significant (n.s.).

Figure 5. Aurora-A Regulates Splicing Factor Activity through Phosphorylation. (**A**) Phosphorylation of SRSF3 by Aurora-A *in vivo*. Left panel: Phosphorylation of SRSF3 was analyzed upon Aurora-A inhibition in Hela cells by Phos-tag gels on the top panel. The western blot analysis of the SRSF3 is shown in the middle panel. TBP was used as a loading control as shown in the bottom panel. Right panel: Phosphorylation of SRSF3 was analyzed upon overexpression of wildtype or kinase-dead mutant (T287A, T288A) of Aurora-A in Hela cells by Phos-tag gels. **(B)** Phosphorylation of SR proteins (SRSF1, SRSF3 and SRSF7) by Aurora-A was analyzed by autoradiography on the top panel. GST was used as a negative control. Coomassie staining of purified recombinant GST-tagged SR

proteins and western blot analysis of the HIS-tagged Aurora-A kinase are shown in the bottom two panels. The orange arrowhead indicates the auto-phosphorylation of Aurora-A and the green arrowhead indicates the phosphorylation of substrate (SR proteins). (**C**) Phosphorylation of hnRNP proteins (HNRNPC and PTBP1) by Aurora-A was analyzed by autoradiography on the top panel. GST was used as a negative control. Western blots of purified recombinant GST-tagged hnRNP proteins and HIS-tagged Aurora-A kinase are shown in the bottom two panels. The orange arrowhead indicates the auto-phosphorylation of Aurora-A and the green arrowhead indicates the phosphorylation of substrate (hnRNP proteins). GST was used as a negative control. (**D**) RT-PCR assays monitoring endogenous splicing of CLK1 exon 4 in HEK293T upon inhibition of Aurora-A with MLN8237 (2μM) for 72 hours. Since the exon 4 skipped isoform undergoes rapid degradation by nonsense-mediated decay (NMD), cycloheximide was applied for the last four hours to inhibit NMD and monitor splicing changes. PSI values are indicated. Two-tailed unpaired t-tests are applied. (**E**) RT-PCR assays monitoring endogenous splicing of CLK1 exon 4 in HEK293T or HeLa cells upon knockdown of Aurora-A, SRSF3, or both for 72 hours. Cycloheximide treatment was performed for the last four hours. PSI values are indicated. Two-tailed unpaired t-tests are applied.

REFERENCES

1. Carmena,M., Earnshaw,W.C. and Glover,D.M. (2015) The Dawn of Aurora Kinase Research: From Fly Genetics to the Clinic. *Front Cell Dev Biol*, **3**, 73.

2. Chan,C.S. and Botstein,D. (1993) Isolation and characterization of chromosome-gain and increase-in-ploidy mutants in yeast. *Genetics*, **135**, 677–691.

3. Francisco,L. and Chan,C.S. (1994) Regulation of yeast chromosome segregation by Ipl1 protein kinase and type 1 protein phosphatase. *Cell Mol Biol Res*, **40**, 207–213.

4. Glover,D.M., Leibowitz,M.H., McLean,D.A. and Parry,H. (1995) Mutations in aurora prevent centrosome separation leading to the formation of monopolar spindles. *Cell*, **81**, 95–105.

5. Roghi,C., Giet,R., Uzbekov,R., Morin,N., Chartrain,I., Le Guellec,R., Couturier,A., Dorée,M., Philippe,M. and Prigent,C. (1998) The Xenopus protein kinase pEg2 associates with the centrosome in a cell cycle-dependent manner, binds to the spindle microtubules and is involved in bipolar mitotic spindle assembly. *J. Cell. Sci.*, **111 (Pt 5)**, 557–572.

6. Sen,S., Zhou,H. and White,R.A. (1997) A putative serine/threonine kinase encoding gene BTAK on chromosome 20q13 is amplified and overexpressed in human breast cancer cell lines. *Oncogene*, **14**, 2195–2200.

7. Kimura,M., Kotani,S., Hattori,T., Sumi,N., Yoshioka,T., Todokoro,K. and Okano,Y. (1997) Cell cycle-dependent expression and spindle pole localization of a novel human protein kinase, Aik, related to Aurora of Drosophila and yeast Ipl1. *J Biol Chem*, **272**, 13766–13771.

8. Yan,M., Wang,C., He,B., Yang,M., Tong,M., Long,Z., Liu,B., Peng,F., Xu,L., Zhang,Y., *et al.* (2016) Aurora-A Kinase: A Potent Oncogene and Target for Cancer Therapy. *Med Res Rev*, **36**, 1036–1079.

9. Reboutier,D., Benaud,C. and Prigent,C. (2015) Aurora A's Functions During Mitotic Exit: The Guess Who Game. *Front Oncol*, **5**, 290.

10. Bertolin,G., Bulteau,A.-L., Alves-Guerra,M.-C., Burel,A., Lavault,M.-T., Gavard,O., Le Bras,S., Gagné,J.-P., Poirier,G.G., Le Borgne,R., *et al.* (2018) Aurora kinase A localises to mitochondria to control organelle dynamics and energy production. *Elife*, **7**.

11. Zheng,F., Yue,C., Li,G., He,B., Cheng,W., Wang,X., Yan,M., Long,Z., Qiu,W., Yuan,Z., *et al.* (2016) Nuclear AURKA acquires kinase-independent transactivating function to enhance breast cancer stem cell phenotype. *Nat Commun*, **7**, 10180.

12. Pascreau,G., Delcros,J.-G., Cremet,J.-Y., Prigent,C. and Arlot-Bonnemains,Y. (2005) Phosphorylation of maskin by Aurora-A participates in the control of sequential protein synthesis during Xenopus laevis oocyte maturation. *J. Biol. Chem.*, **280**, 13415–13423.

13. Berget,S.M., Moore,C. and Sharp,P.A. (1977) Spliced segments at the 5' terminus of adenovirus 2 late mRNA. *Proc. Natl. Acad. Sci. U.S.A.*, **74**, 3171–3175.

14. Chow,L.T., Gelinas,R.E., Broker,T.R. and Roberts,R.J. (1977) An amazing sequence arrangement at the 5' ends of adenovirus 2 messenger RNA. *Cell*, **12**, 1–8.

15. Frendewey,D. and Keller,W. (1985) Stepwise assembly of a pre-mRNA splicing complex requires U-snRNPs and specific intron sequences. *Cell*, **42**, 355–367.

16. Konarska,M.M. and Sharp,P.A. (1986) Electrophoretic separation of complexes involved in the splicing of precursors to mRNAs. *Cell*, **46**, 845–855.

17. Jurica,M.S. and Moore,M.J. (2003) Pre-mRNA splicing: awash in a sea of proteins. *Mol. Cell*, **12**, 5–14.

18. Schmidt,C., Grønborg,M., Deckert,J., Bessonov,S., Conrad,T., Lührmann,R. and Urlaub,H. (2014) Mass spectrometry-based relative quantification of proteins in precatalytic and catalytically active spliceosomes by metabolic labeling (SILAC), chemical labeling (iTRAQ), and label-free spectral count. *RNA*, **20**, 406–420.

19. Wahl,M.C., Will,C.L. and Lührmann,R. (2009) The spliceosome: design principles of a dynamic RNP machine. *Cell*, **136**, 701–718.

20. Dominguez,D., Tsai,Y.-H., Weatheritt,R., Wang,Y., Blencowe,B.J. and Wang,Z. (2016) An extensive program of periodic alternative splicing linked to cell cycle progression. *Elife*, **5**.

21. Tapial,J., Ha,K.C.H., Sterne-Weiler,T., Gohr,A., Braunschweig,U., Hermoso-Pulido,A., Quesnel-Vallières,M., Permanyer,J., Sodaei,R., Marquez,Y., *et al.* (2017) An atlas of alternative splicing profiles and functional associations reveals new regulatory programs and genes that simultaneously express multiple major isoforms. *Genome Res.*, **27**, 1759–1768.

22. Xiao,M.-S., Damodaran,A.P., Kumari,B., Dickson,E., Xing,K., On,T.A., Parab,N., King,H.E., Perez,A.R., Guiblet,W.M., *et al.* (2024) Genome-scale exon perturbation screens uncover exons critical for cell fitness. *Molecular Cell*, **84**, 2553-2572.e19.

23. Agafonov,D.E., Deckert,J., Wolf,E., Odenwälder,P., Bessonov,S., Will,C.L., Urlaub,H. and Lührmann,R. (2011) Semiquantitative proteomic analysis of the human spliceosome via a novel two-dimensional gel electrophoresis method. *Mol. Cell. Biol.*, **31**, 2667–2682.

24. Hegele,A., Kamburov,A., Grossmann,A., Sourlis,C., Wowro,S., Weimann,M., Will,C.L., Pena,V., Lührmann,R. and Stelzl,U. (2012) Dynamic protein-protein interaction wiring of the human spliceosome. *Mol. Cell*, **45**, 567–580.

25. Le Bras,S., Damodaran,A.P. and Le Bras,S. (2018) Aurora A and cancer. *BJSTR*, **3**.

26. Tang,A., Gao,K., Chu,L., Zhang,R., Yang,J. and Zheng,J. (2017) Aurora kinases: novel therapy targets in cancers. *Oncotarget*, **8**, 23937–23954.

27. Wang,X., Zhou,Y.-X., Qiao,W., Tominaga,Y., Ouchi,M., Ouchi,T. and Deng,C.-X. (2006) Overexpression of aurora kinase A in mouse mammary epithelium induces genetic instability preceding mammary tumor formation. *Oncogene*, **25**, 7148–7158.

28. Damodaran,A.P., Vaufrey,L., Gavard,O. and Prigent,C. (2017) Aurora A Kinase Is a Priority Pharmaceutical Target for the Treatment of Cancers. *Trends Pharmacol. Sci.*, **38**, 687–700.

29. Reboutier,D., Troadec,M.-B., Cremet,J.-Y., Chauvin,L., Guen,V., Salaun,P. and Prigent,C. (2013) Aurora A is involved in central spindle assembly through phosphorylation of Ser 19 in P150Glued. *J. Cell Biol.*, **201**, 65–79.

30. Tsai,M.-Y., Wiese,C., Cao,K., Martin,O., Donovan,P., Ruderman,J., Prigent,C. and Zheng,Y. (2003) A Ran signalling pathway mediated by the mitotic kinase Aurora A in spindle assembly. *Nat. Cell Biol.*, **5**, 242–248.

31. Eyers,P.A., Erikson,E., Chen,L.G. and Maller,J.L. (2003) A novel mechanism for activation of the protein kinase Aurora A. *Curr. Biol.*, **13**, 691–697.

32. Vaufrey,L., Damodaran,A.P., Gavard,O., Bras,S.L. and Prigent,C. (2017) Regulation of Aurora Kinases and Their Activity. In Prigent,C. (ed), *Protein Phosphorylation*. InTech.

33. Joukov,V., De Nicolo,A., Rodriguez,A., Walter,J.C. and Livingston,D.M. (2010) Centrosomal protein of 192 kDa (Cep192) promotes centrosome-driven spindle assembly by engaging in organelle-specific Aurora A activation. *Proc. Natl. Acad. Sci. U.S.A.*, **107**, 21022–21027.

34. Zeng,K., Bastos,R.N., Barr,F.A. and Gruneberg,U. (2010) Protein phosphatase 6 regulates mitotic spindle formation by controlling the T-loop phosphorylation state of Aurora A bound to its activator TPX2. *J. Cell Biol.*, **191**, 1315–1332.

35. Katayama,H., Zhou,H., Li,Q., Tatsuka,M. and Sen,S. (2001) Interaction and feedback regulation between STK15/BTAK/Aurora-A kinase and protein phosphatase 1 through mitotic cell division cycle. *J. Biol. Chem.*, **276**, 46219–46224.

36. Lim,N.R., Yeap,Y.Y.C., Zhao,T.T., Yip,Y.Y., Wong,S.C., Xu,D., Ang,C.-S., Williamson,N.A., Xu,Z., Bogoyevitch,M.A., *et al.* (2015) Opposing roles for JNK and Aurora A in regulating the association of WDR62 with spindle microtubules. *J. Cell. Sci.*, **128**, 527–540.

37. Dar,A.A., Belkhiri,A., Ecsedy,J., Zaika,A. and El-Rifai,W. (2008) Aurora kinase A inhibition leads to p73-dependent apoptosis in p53-deficient cancer cells. *Cancer Res.*, **68**, 8998–9004.

38. Moustafa-Kamal,M., Gamache,I., Lu,Y., Li,S. and Teodoro,J.G. (2013) BimEL is phosphorylated at mitosis by Aurora A and targeted for degradation by βTrCP1. *Cell Death Differ.*, **20**, 1393–1403.

39. Jeong,G.U. and Ahn,B.-Y. (2019) Aurora kinase A promotes hepatitis B virus replication and expression. *Antiviral Res.*, **170**, 104572.

40. Grant,R., Abdelbaki,A., Bertoldi,A., Gavilan,M.P., Mansfeld,J., Glover,D.M. and Lindon,C. (2018) Constitutive regulation of mitochondrial morphology by Aurora A kinase depends on a predicted cryptic targeting sequence at the N-terminus. *Open Biol*, **8**.

41. Kashatus,D.F., Lim,K.-H., Brady,D.C., Pershing,N.L.K., Cox,A.D. and Counter,C.M. (2011) RALA and RALBP1 regulate mitochondrial fission at mitosis. *Nat. Cell Biol.*, **13**, 1108–1115.

42. Jones,D., Noble,M., Wedge,S.R., Robson,C.N. and Gaughan,L. (2017) Aurora A regulates expression of AR-V7 in models of castrate resistant prostate cancer. *Sci Rep*, **7**, 40957.

43. Moore,M.J., Wang,Q., Kennedy,C.J. and Silver,P.A. (2010) An alternative splicing network links cell-cycle control to apoptosis. *Cell*, **142**, 625–636.

44. Arslanhan,M.D., Rauniyar,N., Yates,J.R. and Firat-Karalar,E.N. (2021) Aurora Kinase A proximity map reveals centriolar satellites as regulators of its ciliary function. *EMBO Reports*, **22**.

45. Wahl,M.C. and Lührmann,R. (2015) SnapShot: Spliceosome Dynamics I. *Cell*, **161**, 1474-e1.

46. Coelho,M.B. and Smith,C.W.J. (2014) Regulation of alternative pre-mRNA splicing. *Methods Mol. Biol.*, **1126**, 55–82.

47. Fu,X.-D. and Ares,M. (2014) Context-dependent control of alternative splicing by RNA-binding proteins. *Nat. Rev. Genet.*, **15**, 689–701.

48. Spector,D.L. and Lamond,A.I. (2011) Nuclear speckles. *Cold Spring Harb Perspect Biol*, **3**.

49. Dopie,J., Sweredoski,M.J., Moradian,A. and Belmont,A.S. (2020) Tyramide signal amplification mass spectrometry (TSA-MS) ratio identifies nuclear speckle proteins. *J Cell Biol*, **219**, e201910207.

50. Cléry,A. and Allain,F.H.-T. (2013) FROM STRUCTURE TO FUNCTION OF RNA BINDING DOMAINS Landes Bioscience.

51. Park,J.-H., Jong,H.-S., Kim,S.G., Jung,Y., Lee,K.-W., Lee,J.-H., Kim,D.-K., Bang,Y.-J. and Kim,T.-Y. (2008) Inhibitors of histone deacetylases induce tumor-selective cytotoxicity through modulating Aurora-A kinase. *J. Mol. Med.*, **86**, 117–128.

52. Yang,H., Burke,T., Dempsey,J., Diaz,B., Collins,E., Toth,J., Beckmann,R. and Ye,X. (2005) Mitotic requirement for aurora A kinase is bypassed in the absence of aurora B kinase. *FEBS Lett.*, **579**, 3385–3391.

53. Asteriti,I.A., Di Cesare,E., De Mattia,F., Hilsenstein,V., Neumann,B., Cundari,E., Lavia,P. and Guarguaglini,G. (2014) The Aurora-A inhibitor MLN8237 affects multiple mitotic processes and induces dose-dependent mitotic abnormalities and aneuploidy. *Oncotarget*, **5**, 6229–6242.

54. Robinson,M.D., McCarthy,D.J. and Smyth,G.K. (2010) edgeR: a Bioconductor package for differential expression analysis of digital gene expression data. *Bioinformatics*, **26**, 139–140.

55. Irimia,M., Weatheritt,R.J., Ellis,J.D., Parikshak,N.N., Gonatopoulos-Pournatzis,T., Babor,M., Quesnel-Vallières,M., Tapial,J., Raj,B., O'Hanlon,D., *et al.* (2014) A highly conserved program of neuronal microexons is misregulated in autistic brains. *Cell*, **159**, 1511–1523.

56. Carazo-Salas,R.E., Guarguaglini,G., Gruss,O.J., Segref,A., Karsenti,E. and Mattaj,I.W. (1999) Generation of GTP-bound Ran by RCC1 is required for chromatin-induced mitotic spindle formation. *Nature*, **400**, 178–181.

57. Tissir,F., Qu,Y., Montcouquiol,M., Zhou,L., Komatsu,K., Shi,D., Fujimori,T., Labeau,J., Tyteca,D., Courtoy,P., *et al.* (2010) Lack of cadherins Celsr2 and Celsr3 impairs ependymal ciliogenesis, leading to fatal hydrocephalus. *Nat Neurosci*, **13**, 700–707.

58. Dutertre,S., Cazales,M., Quaranta,M., Froment,C., Trabut,V., Dozier,C., Mirey,G., Bouché,J.-P., Theis-Febvre,N., Schmitt,E., *et al.* (2004) Phosphorylation of CDC25B by Aurora-A at the centrosome contributes to the G2-M transition. *J. Cell. Sci.*, **117**, 2523–2531.

59. Pugacheva,E.N., Jablonski,S.A., Hartman,T.R., Henske,E.P. and Golemis,E.A. (2007) HEF1-dependent Aurora A activation induces disassembly of the primary cilium. *Cell*, **129**, 1351–1363.

60. Seki,A., Coppinger,J.A., Jang,C.-Y., Yates,J.R. and Fang,G. (2008) Bora and the kinase Aurora a cooperatively activate the kinase Plk1 and control mitotic entry. *Science*, **320**, 1655–1658.

61. Dominguez,D., Tsai,Y.-H., Gomez,N., Jha,D.K., Davis,I. and Wang,Z. (2016) A high-resolution transcriptome map of cell cycle reveals novel connections between periodic genes and cancer. *Cell Res*, **26**, 946–962.

62. Gohr,A. and Irimia,M. (2019) Matt: Unix tools for alternative splicing analysis. *Bioinformatics (Oxford, England)*, **35**, 130–132.

63. Singh,R., Valcárcel,J. and Green,M.R. (1995) Distinct binding specificities and functions of higher eukaryotic polypyrimidine tract-binding proteins. *Science*, **268**, 1173–1176.

64. Naro,C. and Sette,C. (2013) Phosphorylation-mediated regulation of alternative splicing in cancer. *Int J Cell Biol*, **2013**, 151839.

65. Allemand,E., Guil,S., Myers,M., Moscat,J., Cáceres,J.F. and Krainer,A.R. (2005) Regulation of heterogenous nuclear ribonucleoprotein A1 transport by phosphorylation in cells stressed by osmotic shock. *Proc. Natl. Acad. Sci. U.S.A.*, **102**, 3605–3610.

66. Misteli,T. and Spector,D.L. (1999) RNA polymerase II targets pre-mRNA splicing factors to transcription sites in vivo. *Mol. Cell*, **3**, 697–705.

67. Misteli,T., Cáceres,J.F., Clement,J.Q., Krainer,A.R., Wilkinson,M.F. and Spector,D.L. (1998) Serine phosphorylation of SR proteins is required for their recruitment to sites of transcription in vivo. *J. Cell Biol.*, **143**, 297–307.

68. Xiao,S.H. and Manley,J.L. (1997) Phosphorylation of the ASF/SF2 RS domain affects both protein-protein and protein-RNA interactions and is necessary for splicing. *Genes Dev.*, **11**, 334–344.

69. Liu,B., Anderson,S.L., Qiu,J. and Rubin,B.Y. (2013) Cardiac glycosides correct aberrant splicing of IKBKAP-encoded mRNA in familial dysautonomia derived cells by suppressing expression of SRSF3. *The FEBS Journal*, **280**, 3632–3646.

70. Ninomiya,K., Kataoka,N. and Hagiwara,M. (2011) Stress-responsive maturation of Clk1/4 pre-mRNAs promotes phosphorylation of SR splicing factor. *J Cell Biol*, **195**, 27–40.

71. Wahl,M.C. and Lührmann,R. (2015) SnapShot: Spliceosome Dynamics II. *Cell*, **162**, 456-456.e1.

72. Hsueh,K.-W., Fu,S.-L., Huang,C.-Y.F. and Lin,C.-H. (2011) Aurora-A phosphorylates hnRNPK and disrupts its interaction with p53. *FEBS Lett.*, **585**, 2671–2675.

73. Ma,N., Matsunaga,S., Morimoto,A., Sakashita,G., Urano,T., Uchiyama,S. and Fukui,K. (2011) The nuclear scaffold protein SAF-A is required for kinetochore-microtubule attachment and contributes to the targeting of Aurora-A to mitotic spindles. *J. Cell. Sci.*, **124**, 394–404.

74. Cordin,O. and Beggs,J.D. (2013) RNA helicases in splicing. *RNA Biol*, **10**, 83–95.

75. De,I., Schmitzová,J. and Pena,V. (2016) The organization and contribution of helicases to RNA splicing. *Wiley Interdiscip Rev RNA*, **7**, 259–274.

76. Gilman,B., Tijerina,P. and Russell,R. (2017) Distinct RNA-unwinding mechanisms of DEAD-box and DEAH-box RNA helicase proteins in remodeling structured RNAs and RNPs. *Biochem Soc Trans*, **45**, 1313–1321.

77. Liu,Y.-C. and Cheng,S.-C. (2015) Functional roles of DExD/H-box RNA helicases in Pre-mRNA splicing. *J Biomed Sci*, **22**, 54.

78. Chan,S.-P. and Cheng,S.-C. (2005) The Prp19-associated complex is required for specifying interactions of U5 and U6 with pre-mRNA during spliceosome activation. *J Biol Chem*, **280**, 31190–31199.

79. Song,E.J., Werner,S.L., Neubauer,J., Stegmeier,F., Aspden,J., Rio,D., Harper,J.W., Elledge,S.J., Kirschner,M.W. and Rape,M. (2010) The Prp19 complex and the Usp4Sart3 deubiquitinating enzyme control reversible ubiquitination at the spliceosome. *Genes Dev*, **24**, 1434–1447.

80. Aviner,R., Hofmann,S., Elman,T., Shenoy,A., Geiger,T., Elkon,R., Ehrlich,M. and Elroy-Stein,O. (2017) Proteomic analysis of polyribosomes identifies splicing factors as potential regulators of translation during mitosis. *Nucleic Acids Res*, **45**, 5945–5957.

81. Chanarat,S. and Sträßer,K. (2013) Splicing and beyond: the many faces of the Prp19 complex. *Biochim Biophys Acta*, **1833**, 2126–2134.

82. Kędzierska,H. and Piekiełko-Witkowska,A. (2017) Splicing factors of SR and hnRNP families as regulators of apoptosis in cancer. *Cancer Lett*, **396**, 53–65.

83. Robert,F. and Pelletier,J. (2013) Perturbations of RNA helicases in cancer. *Wiley Interdiscip Rev RNA*, **4**, 333–349.

84. Misteli,T., Cáceres,J.F. and Spector,D.L. (1997) The dynamics of a pre-mRNA splicing factor in living cells. *Nature*, **387**, 523–527.

85. Kettenbach,A.N., Schweppe,D.K., Faherty,B.K., Pechenick,D., Pletnev,A.A. and Gerber,S.A. (2011) Quantitative phosphoproteomics identifies substrates and functional modules of Aurora and Polo-like kinase activities in mitotic cells. *Sci Signal*, **4**, rs5.

86. Naro,C., Barbagallo,F., Chieffi,P., Bourgeois,C.F., Paronetto,M.P. and Sette,C. (2014) The centrosomal kinase NEK2 is a novel splicing factor kinase involved in cell survival. *Nucleic Acids Res.*, **42**, 3218–3227.

87. Blaustein,M., Pelisch,F., Tanos,T., Muñoz,M.J., Wengier,D., Quadrana,L., Sanford,J.R., Muschietti,J.P., Kornblihtt,A.R., Cáceres,J.F., *et al.* (2005) Concerted regulation of nuclear and cytoplasmic activities of SR proteins by AKT. *Nat. Struct. Mol. Biol.*, **12**, 1037–1044.

88. Weg-Remers,S., Ponta,H., Herrlich,P. and König,H. (2001) Regulation of alternative pre-mRNA splicing by the ERK MAP-kinase pathway. *EMBO J.*, **20**, 4194–4203.

89. Paronetto,M.P., Achsel,T., Massiello,A., Chalfant,C.E. and Sette,C. (2007) The RNA-binding protein Sam68 modulates the alternative splicing of Bcl-x. *J. Cell Biol.*, **176**, 929–939.

90. Patel,N.A., Kaneko,S., Apostolatos,H.S., Bae,S.S., Watson,J.E., Davidowitz,K., Chappell,D.S., Birnbaum,M.J., Cheng,J.Q. and Cooper,D.R. (2005) Molecular and genetic studies imply Akt-mediated signaling promotes protein kinase CbetaII alternative splicing via phosphorylation of serine/arginine-rich splicing factor SRp40. *J. Biol. Chem.*, **280**, 14302–14309.

91. Kvissel,A.-K., Ørstavik,S., Eikvar,S., Brede,G., Jahnsen,T., Collas,P., Akusjärvi,G. and Skålhegg,B.S. (2007) Involvement of the catalytic subunit of protein kinase A and of HA95 in pre-mRNA splicing. *Exp. Cell Res.*, **313**, 2795–2809.

92. Johnson,J.L., Yaron,T.M., Huntsman,E.M., Kerelsky,A., Song,J., Regev,A., Lin,T.-Y., Liberatore,K., Cizin,D.M., Cohen,B.M., *et al.* (2023) An atlas of substrate specificities for the human serine/threonine kinome. *Nature*, **613**, 759–766.

93. Cromm,P.M., Spiegel,J., Grossmann,T.N. and Waldmann,H. (2015) Direct Modulation of Small GTPase Activity and Function. *Angew. Chem. Int. Ed.*, **54**, 13516–13537.

94. Eguether,T. and Hahne,M. (2018) Mixed signals from the cell's antennae: primary cilia in cancer. *EMBO Rep*, **19**.

95. Prieto-Dominguez,N., Parnell,C. and Teng,Y. (2019) Drugging the Small GTPase Pathways in Cancer Treatment: Promises and Challenges. *Cells*, **8**.

96. Stark,G.R. and Taylor,W.R. (2006) Control of the G2/M transition. *Mol Biotechnol*, **32**, 227–248.

97. Li,S., Qi,Y., Yu,J., Hao,Y., Xu,L., Ding,X., Zhang,M. and Geng,J. (2023) Aurora kinase A regulates cancer-associated RNA aberrant splicing in breast cancer. *Heliyon*, **9**, e17386.

98. Thomas,J.D., Polaski,J.T., Feng,Q., De Neef,E.J., Hoppe,E.R., McSharry,M.V., Pangallo,J., Gabel,A.M., Belleville,A.E., Watson,J., *et al.* (2020) RNA isoform screens uncover the essentiality and tumor-suppressor activity of ultraconserved poison exons. *Nat Genet*, **52**, 84–94.

99. Aregger,M., Xing,K. and Gonatopoulos-Pournatzis,T. (2021) Application of CHyMErA Cas9-Cas12a combinatorial genome-editing platform for genetic interaction mapping and gene fragment deletion screening. *Nat Protoc*, **16**, 4722–4765.

100. Gonatopoulos-Pournatzis,T., Aregger,M., Brown,K.R., Farhangmehr,S., Braunschweig,U., Ward,H.N., Ha,K.C.H., Weiss,A., Billmann,M., Durbic,T., *et al.* (2020) Genetic interaction mapping and exon-resolution functional genomics with a hybrid Cas9-Cas12a platform. *Nat. Biotechnol.*, **38**, 638–648.

101. Li,J.D., Taipale,M. and Blencowe,B.J. (2024) Efficient, specific, and combinatorial control of endogenous exon splicing with dCasRx-RBM25. *Molecular Cell*, **84**, 2573-2589.e5.

102. Bertolin,G., Alves-Guerra,M.-C., Cheron,A., Burel,A., Prigent,C., Le Borgne,R. and Tramier,M. (2021) Mitochondrial Aurora kinase A induces mitophagy by interacting with MAP1LC3 and Prohibitin 2. *Life Sci Alliance*, **4**, e202000806.

103. Adhikari,B., Bozilovic,J., Diebold,M., Schwarz,J.D., Hofstetter,J., Schröder,M., Wanior,M., Narain,A., Vogt,M., Dudvarski Stankovic,N., *et al.* (2020) PROTAC-mediated degradation reveals a non-catalytic function of AURORA-A kinase. *Nat Chem Biol*, **16**, 1179–1188.

104. Wang,R., Ascanelli,C., Abdelbaki,A., Fung,A., Rasmusson,T., Michaelides,I., Roberts,K. and Lindon,C. (2021) Selective targeting of non-centrosomal AURKA functions through use of a targeted protein degradation tool. *Commun Biol*, **4**, 640.

105. Fu,Y., Huang,B., Shi,Z., Han,J., Wang,Y., Huangfu,J. and Wu,W. (2013) SRSF1 and SRSF9 RNA binding proteins promote Wnt signalling-mediated tumorigenesis by enhancing β-catenin biosynthesis. *EMBO Mol Med*, **5**, 737–750.

106. Juillard,F., Bazot,Q., Mure,F., Tafforeau,L., Macri,C., Rabourdin-Combe,C., Lotteau,V., Manet,E. and Gruffat,H. (2012) Epstein-Barr virus protein EB2 stimulates cytoplasmic mRNA accumulation by counteracting the deleterious effects of SRp20 on viral mRNAs. *Nucleic Acids Res.*, **40**, 6834–6849.

107. Kim,J., Park,R.Y., Chen,J.-K., Kim,J., Jeong,S. and Ohn,T. (2014) Splicing factor SRSF3 represses the translation of programmed cell death 4 mRNA by associating with the 5′-UTR region. *Cell Death Differ*, **21**, 481–490.

108. Cremet,J.Y., Descamps,S., Vérite,F., Martin,A. and Prigent,C. (2003) Preparation and characterization of a human aurora-A kinase monoclonal antibody. *Mol. Cell. Biochem.*, **243**, 123–131.

109. Raudvere,U., Kolberg,L., Kuzmin,I., Arak,T., Adler,P., Peterson,H. and Vilo,J. (2019) g:Profiler: a web server for functional enrichment analysis and conversions of gene lists (2019 update). *Nucleic Acids Res.*, **47**, W191–W198.

110. Merico,D., Isserlin,R., Stueker,O., Emili,A. and Bader,G.D. (2010) Enrichment map: a network-based method for gene-set enrichment visualization and interpretation. *PLoS ONE*, **5**, e13984.

111. Shannon,P., Markiel,A., Ozier,O., Baliga,N.S., Wang,J.T., Ramage,D., Amin,N., Schwikowski,B. and Ideker,T. (2003) Cytoscape: a software environment for integrated models of biomolecular interaction networks. *Genome Res.*, **13**, 2498–2504.

112. Kucera,M., Isserlin,R., Arkhangorodsky,A. and Bader,G.D. (2016) AutoAnnotate: A Cytoscape app for summarizing networks with semantic annotations. *F1000Res*, **5**, 1717.

113. Huang,D.W., Sherman,B.T. and Lempicki,R.A. (2009) Bioinformatics enrichment tools: paths toward the comprehensive functional analysis of large gene lists. *Nucleic Acids Res.*, **37**, 1–13.

114. Huang,D.W., Sherman,B.T. and Lempicki,R.A. (2009) Systematic and integrative analysis of large gene lists using DAVID bioinformatics resources. *Nat Protoc*, **4**, 44–57.

115. Doncheva,N.T., Morris,J.H., Gorodkin,J. and Jensen,L.J. (2019) Cytoscape StringApp: Network Analysis and Visualization of Proteomics Data. *J. Proteome Res.*, **18**, 623–632.

116. Bader,G.D. and Hogue,C.W.V. (2003) An automated method for finding molecular complexes in large protein interaction networks. *BMC Bioinformatics*, **4**, 2.

117. Deutsch,E.W., Csordas,A., Sun,Z., Jarnuczak,A., Perez-Riverol,Y., Ternent,T., Campbell,D.S., Bernal-Llinares,M., Okuda,S., Kawano,S., *et al.* (2017) The ProteomeXchange consortium in 2017: supporting the cultural change in proteomics public data deposition. *Nucleic Acids Res*, **45**, D1100–D1106.

118. Perez-Riverol,Y., Csordas,A., Bai,J., Bernal-Llinares,M., Hewapathirana,S., Kundu,D.J., Inuganti,A., Griss,J., Mayer,G., Eisenacher,M., *et al.* (2019) The PRIDE database and related tools and resources in 2019: improving support for quantification data. *Nucleic Acids Res*, **47**, D442–D450.

119. Edgar,R., Domrachev,M. and Lash,A.E. (2002) Gene Expression Omnibus: NCBI gene expression and hybridization array data repository. *Nucleic Acids Res*, **30**, 207–210.

Figure-1

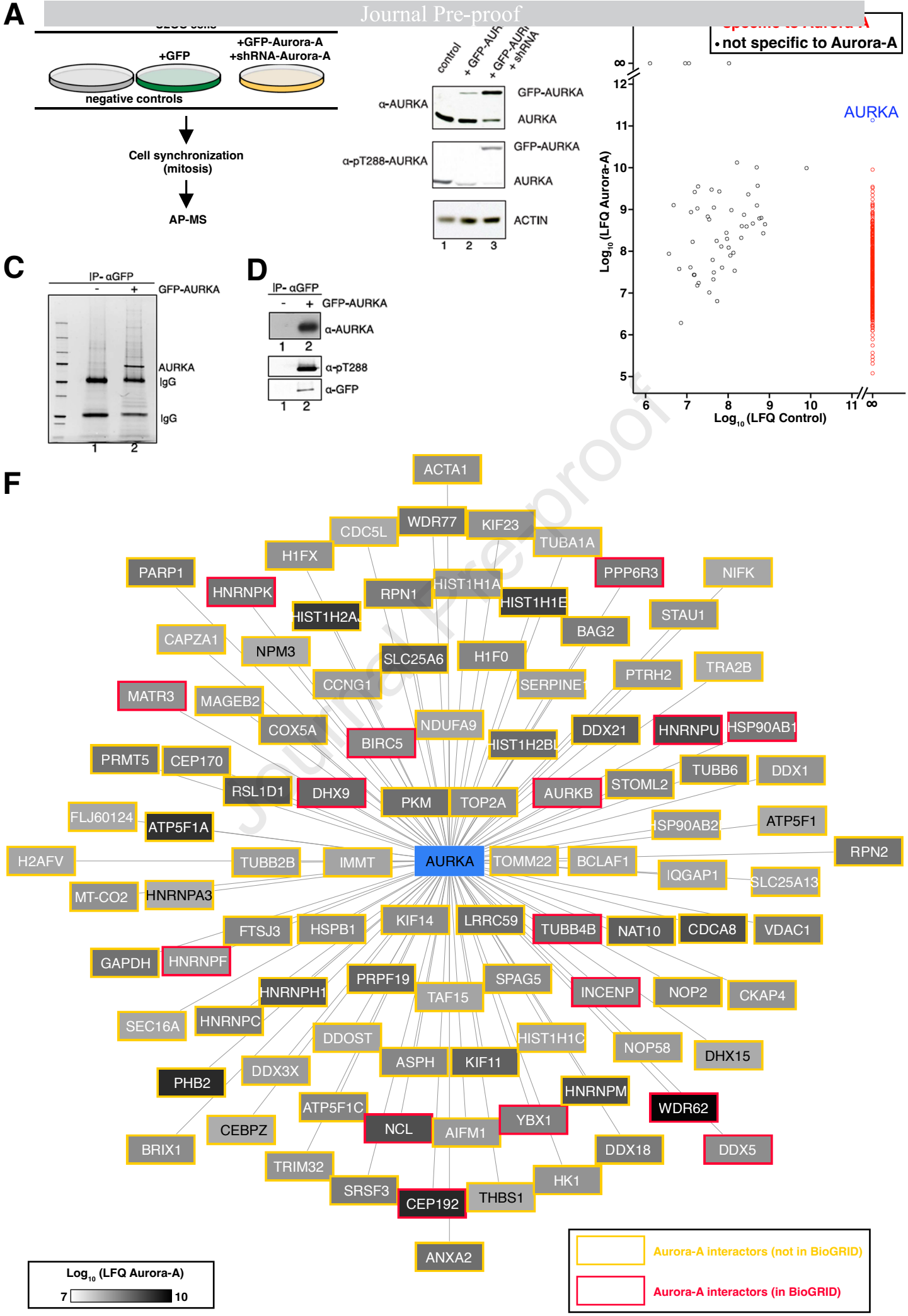

Figure-2

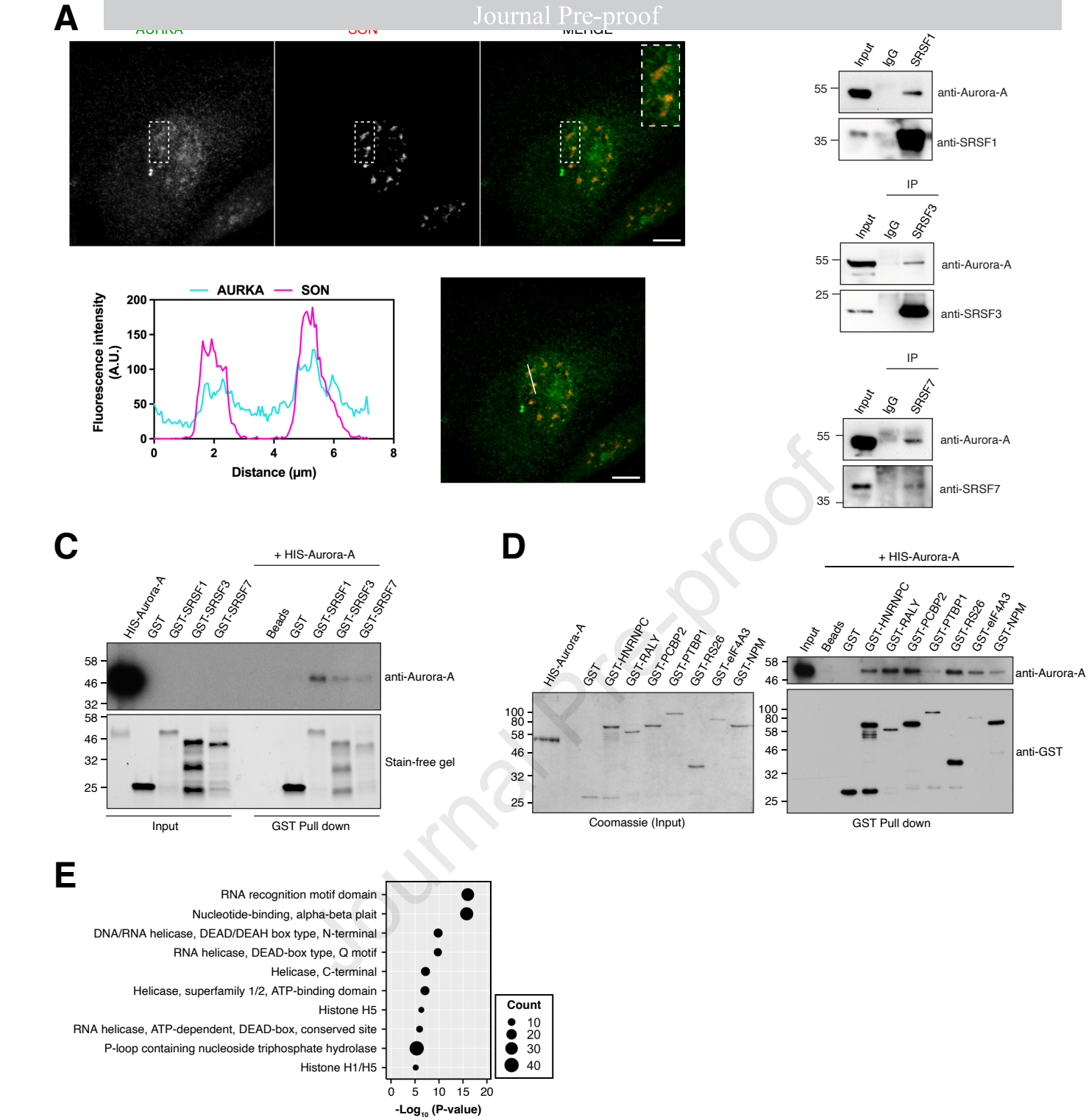

Figure-3

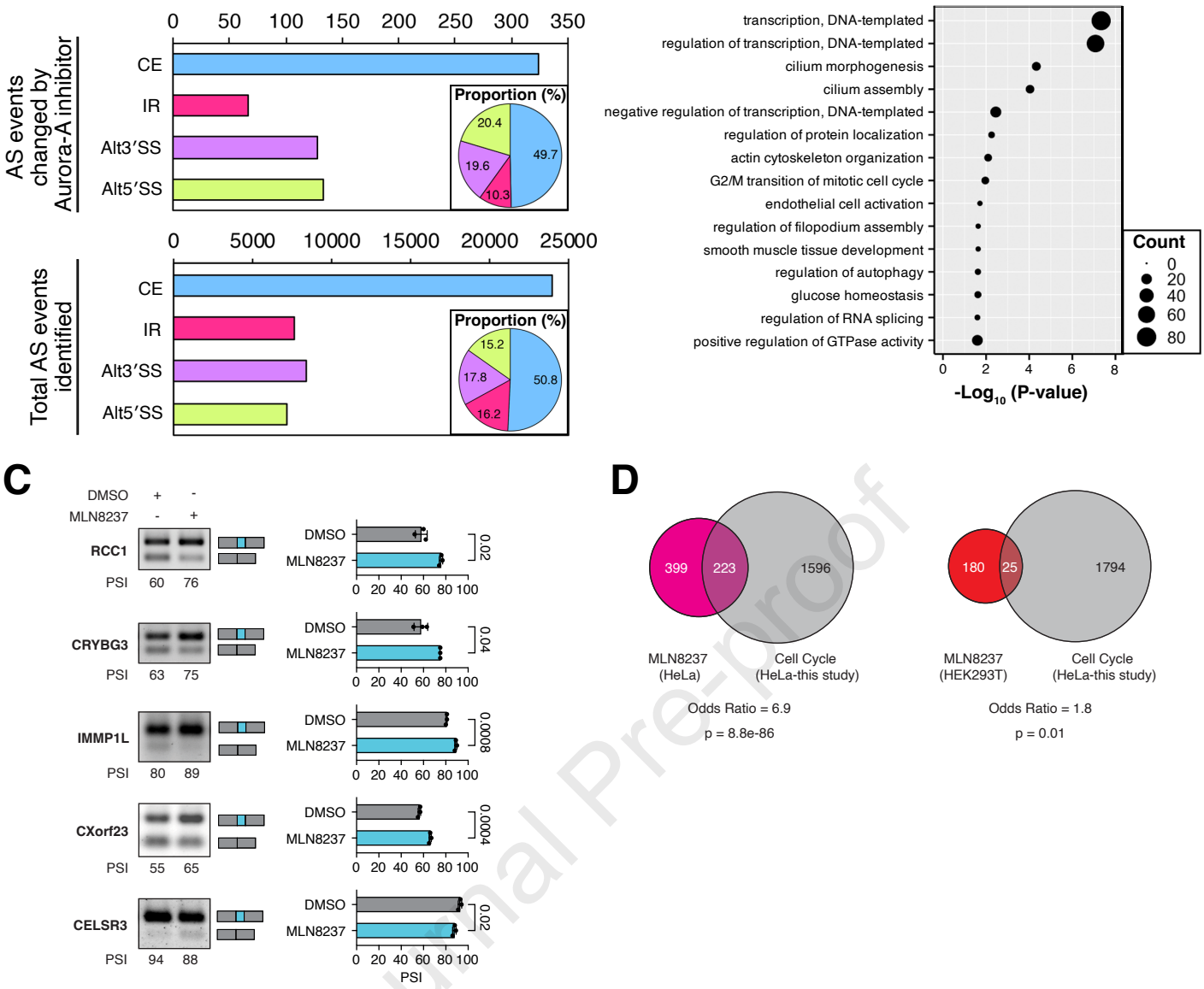

Figure-4

A

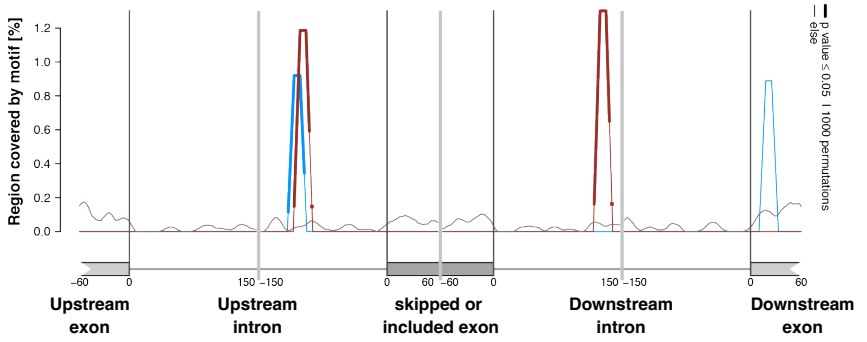

Family	Splicing factors	CISBP-RNA motif	IUPAC	Domain
SR proteins	SRSF1	M105	GGASGRV	RRM
		M154	GGRGGAV	
		M270	GAAGAA	
		M272	RGAAGAAC	
		M273	ACGCGCA	
	SRSF2	M070	GGAGWD	RRM
		M274	GUUCGAGUA	
		M332	UGUUCSAGWU	
		M352	AGSAGAGUA	
	SRSF7	M071	ACGACG	RRM
	SRSF9	M065	KGRWGSM	RRM
		M333	AGGAY	
hnRNP proteins	HNRNPA1	M022	DUAGGGW	RRM
	HNRNPAB	M210	WRGWUAG	RRM
	HNRNPA2B1	M024	DUAGGGW	RRM
	HNRNPC	M025	HUUUUUK	RRM
	RALY	M150	UUUUUUB	RRM
	PCBP2	M043	CCYYCCH	KH
	HNRNPH2	M151	GGGAGGG	RRM
	PTBP1	M228	HYUUUYU	RRM
	HNRNPK	M026	CCAWMCC	KH

B

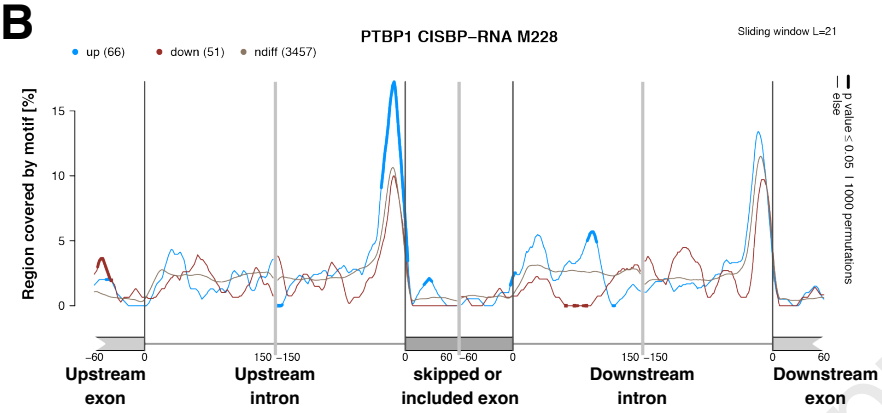

C

D

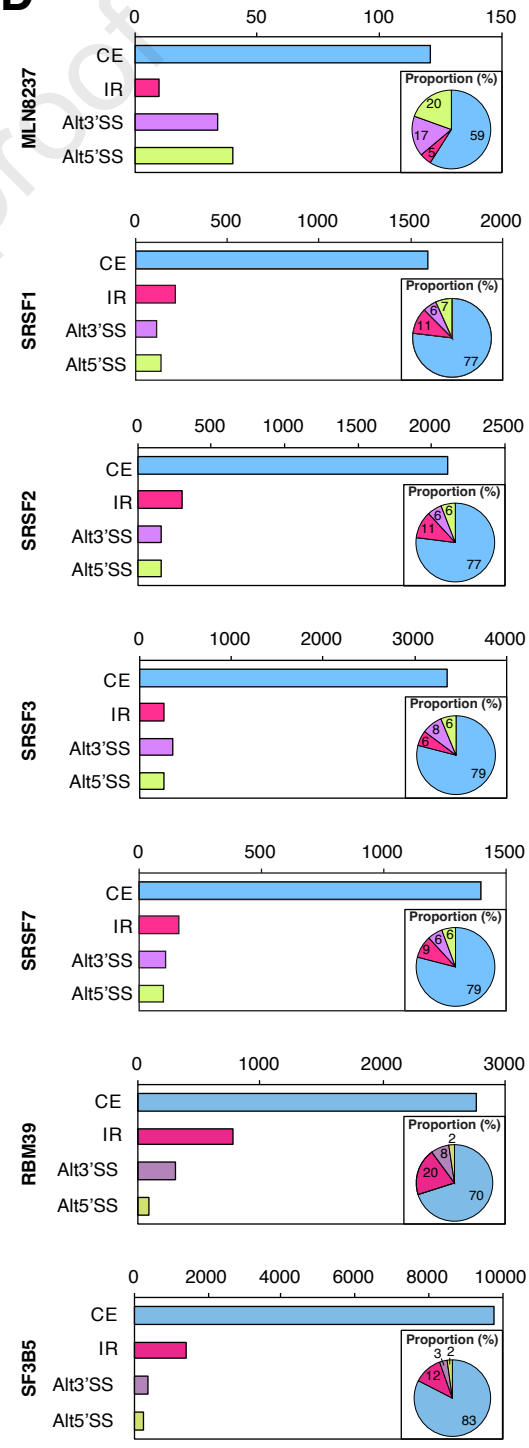

E

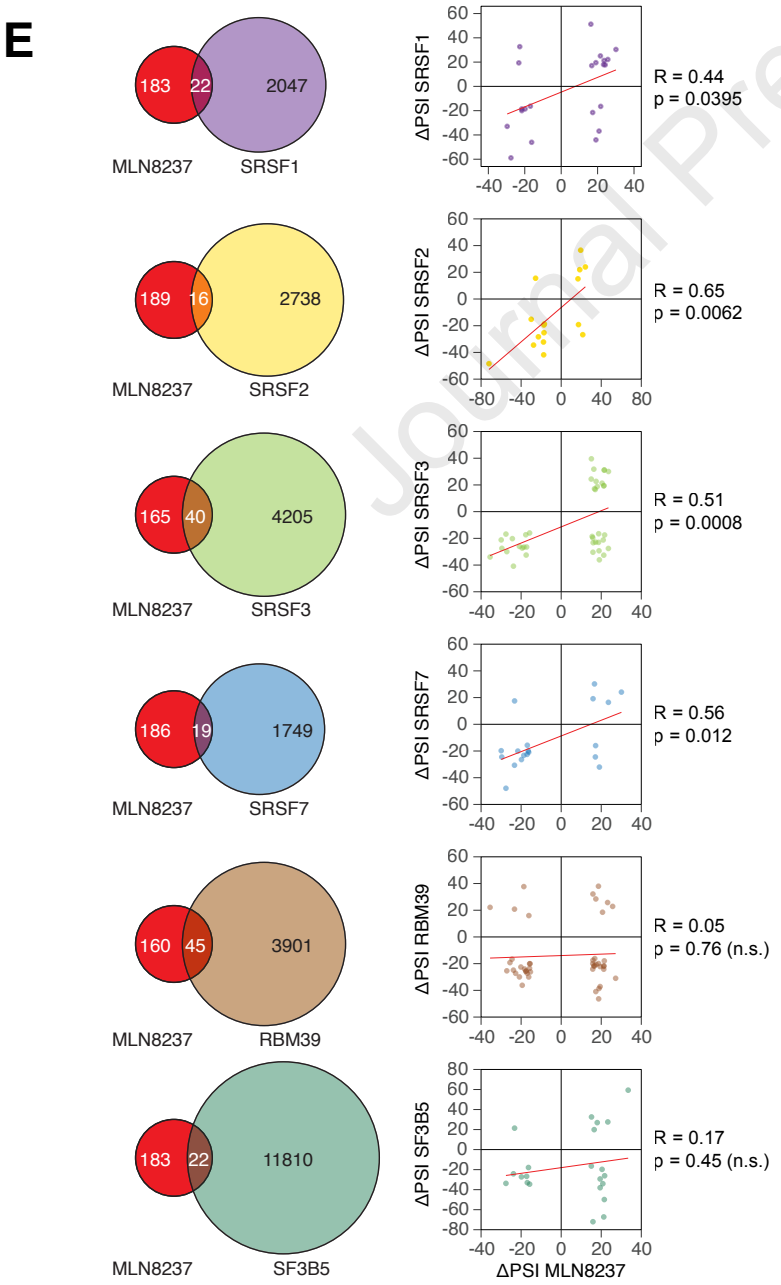

Figure-5

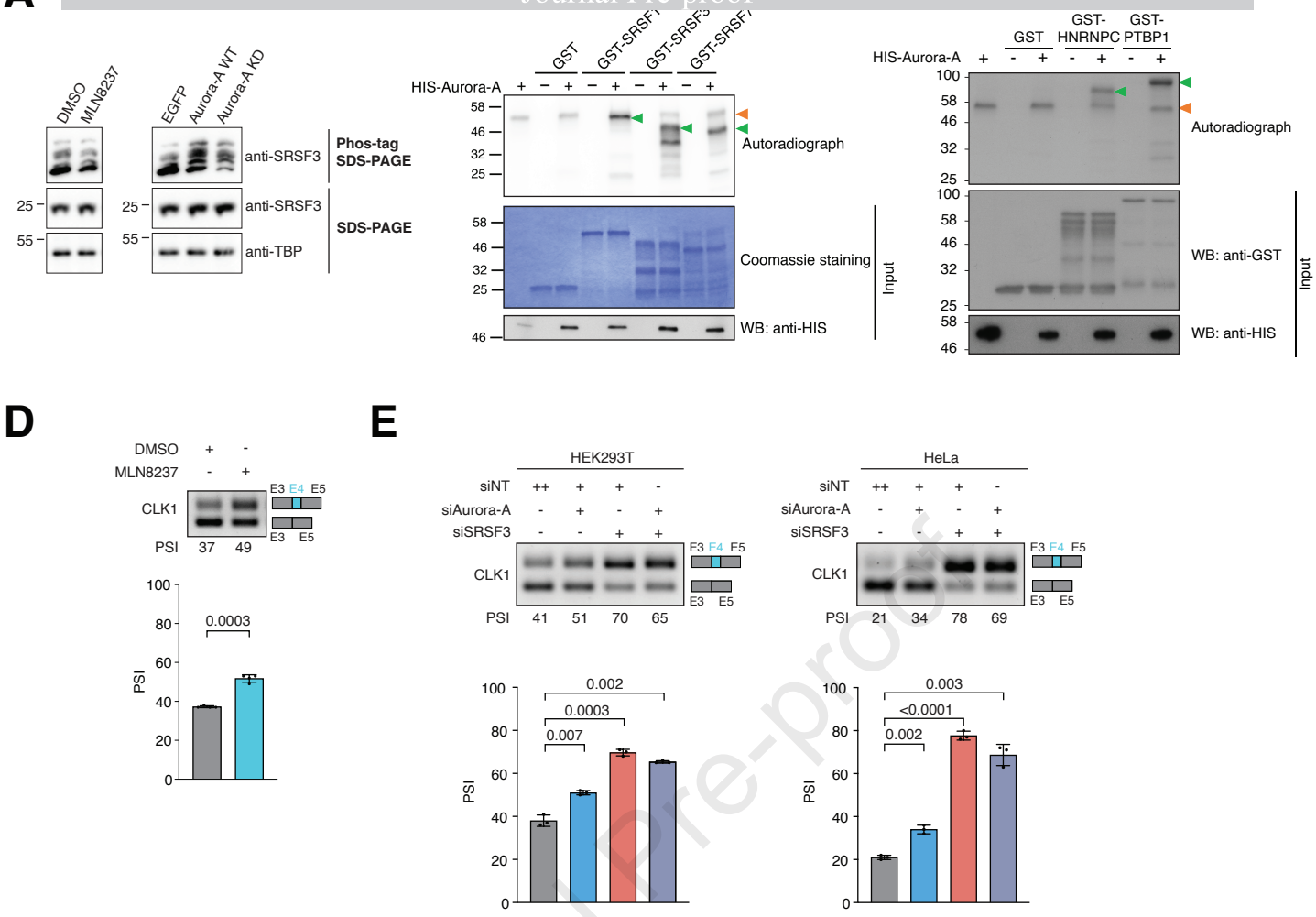

Declaration of interests

☒ The authors declare that they have no known competing financial interests or personal relationships that could have appeared to influence the work reported in this paper.

☐The authors declare the following financial interests/personal relationships which may be considered as potential competing interests: